Table 2. The amino acid difference in prM proteins between the parental virus and the plasmids used in this study

The non-conserved amino acid in the sequence is shown in non-bold.

Virus/ mutant	Position*								
	62	63	64	65	66	67	68	69	70
TBEV (pCAG-TBEME and Oshima-IC)									
Wild type	**E**	**P**	**V**	**D**	**V**	**D**	**C**	**F**	**C**
prE62A	A	–	–	–	–	–	–	–	–
prP63A	–	A	–	–	–	–	–	–	–
prD65A	–	–	–	A	–	–	–	–	–
prV66A	–	–	–	–	A	–	–	–	–
prD67A	–	–	–	–	–	A	–	–	–
prF69A	–	–	–	–	–	–	–	A	–
prV66I	–	–	–	–	I	–	–	–	–
prF69W	–	–	–	–	–	–	–	W	–
	Position†								
	61	**62**	**63**	**64**	**65**	**66**	**67**	**68**	**69**
JEV (pcJEME)									
Wild type	**D**	**P**	**E**	**D**	**V**	**D**	**C**	**W**	**C**
prP62A	–	A	–	–	–	–	–	–	–
prD64A	–	–	–	A	–	–	–	–	–
prV65A	–	–	–	–	A	–	–	–	–
prD66A	–	–	–	–	–	A	–	–	–
prW68A	–	–	–	–	–	–	–	A	–

*Based on TBEV strain Oshima 5-10 (GenBank accession no. AB062063).
†Based on JEV strain Nakayama (GenBank accession no. EF571853).

valine-to-isoleucine substitution was engineered in pCAG-TBEME. Unlike the alanine substitution, the isoleucine substitution did not affect secretion of the E protein, indicating the importance of the branched-chain amino acid at this residue. At position 69, the aromatic amino acid phenylalanine is conserved in tick-borne and no-known-vector flaviviruses, whilst tryptophan is conserved here in mosquito-borne flaviviruses. A phenylalanine-to-tryptophan substitution was engineered at this residue in pCAG-TBEME and this substitution reduced secretion of the E protein.

To confirm the importance of the conserved region in other flaviviruses, similar alanine substitutions were engineered in the pcJEME plasmid expressing the prM and E proteins of JEV. pcJEME plasmids containing the different mutations were transfected into 293T cells. After incubation for 24 h, intracellular and extracellular E proteins were detected by Western blotting. The substitutions of proline-62, aspartate-64, valine-65, aspartate-66 and tryptophan-68 in the prM protein resulted in reduced secretion of the E protein, as observed in TBEV (Fig. 1b). These data indicated that the conserved region in the prM protein of flaviviruses has an important role in the assembly and secretion of the virus particles.

Effect of mutations in the conserved region on prM–E interaction

Interaction between the prM and E proteins is necessary for assembly of the virus particle. To investigate whether the mutations in the conserved region affected the prM–E association, 293T cells transfected with the pCAG-TBEME plasmids were lysed, and co-immunoprecipitation of the prM and E proteins was carried out. As shown in Fig. 2, prM and E proteins were detected in eluates from co-immunoprecipitation samples from cells transfected with pCAG-TBEME carrying the prP63A, prD65A, prV66A or prF69A mutation and in the wild-type plasmid. These data demonstrated that heterodimerization between prM and E was not disrupted by mutations at positions 63, 65, 66 or 69. Following alanine substitution at position 67 (aspartate to alanine), prM and E proteins were not co-immunoprecipitated, indicating that this mutation critically affected the prM–E interaction.

Effect of mutations in the conserved region on intracellular localization

To evaluate whether the mutations in the conserved region affected the intracellular distribution of viral proteins, cells

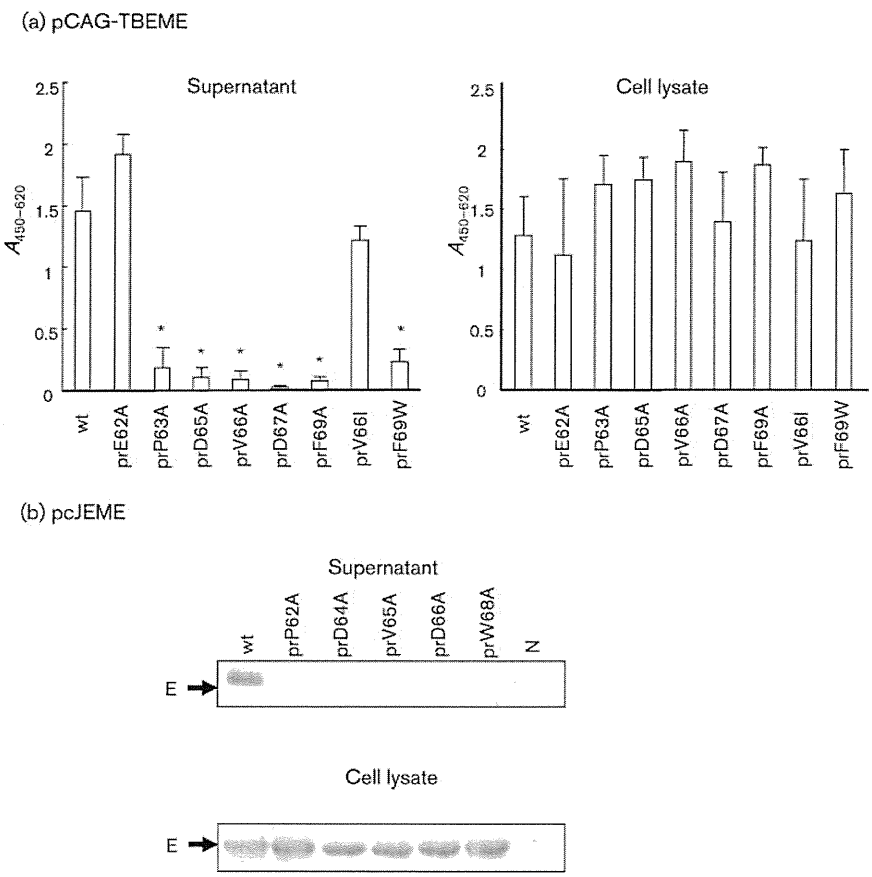

Fig. 1. Mutations in the conserved region of prM reduce the secretion of SPs. PrM and E proteins were expressed in 293T cells by transfection of wild-type (wt) pCAG-TBEME (a) or pcJEME (b) with or without a mutation in the conserved region in prM. After a 24 h incubation, E protein in the solubilized sample was detected by ELISA using TBEV E-specific mAb (a) or Western blotting using JEV E-specific mAb (b). Mean absorbance values (±SD) were calculated from triplicate experiments. Asterisks indicate statistically significant differences compared with the wild-type (wt) plasmid (Student's *t*-test, $P<0.05$). N, Non-transfected control.

transfected with each pCAG-TBEME plasmid were double-stained for TBEV proteins and cellular marker antigens. The distribution of viral proteins in the ER was not affected by the mutations in prM (Fig. 3a). However, whilst the distribution of viral proteins in the Golgi complex was observed in the wild-type-transfected cells, co-localization of viral proteins and Golgi markers was low with the prM protein containing mutations (Fig. 3b). Co-localization of prM and E proteins was similar in all pCAG-TBEME-transfected cells (see Supplementary Fig. S1, available in JGV Online). These data suggested that the mutation in the conserved region of prM caused a defect in the transport of the viral protein to the Golgi complex.

Ultrastructural analysis of particle assembly by prM mutations

To examine whether the mutations in prM affected the assembly of SPs, electron microscope analysis of pCAG-TBEME-transfected cells was performed. As shown in Fig. 4, spherical SPs were observed in the lumen of membrane-bound vesicles in wild-type-transfected cells (Fig. 4a, b). In contrast, filamentous structures were observed in the lumen of membrane-bound vesicles in cells transfected with pCAG-TBEME containing the prP63A, prD65A, prV66A or prF69A mutation (Fig. 4c–f). The filamentous structures were 30–40 nm in width and 0.1 to >1.0 μm in length and had constrictions every 50–100 nm. In prD67A-transfected cells, no SPs or filamentous structures were detected (Fig. 4g). These results indicated that the conserved region of prM has important roles in virion assembly.

Effect of mutations in the conserved region on viral multiplication

To confirm the effect of mutations in prM on viral multiplication, alanine substitutions affecting the secretion

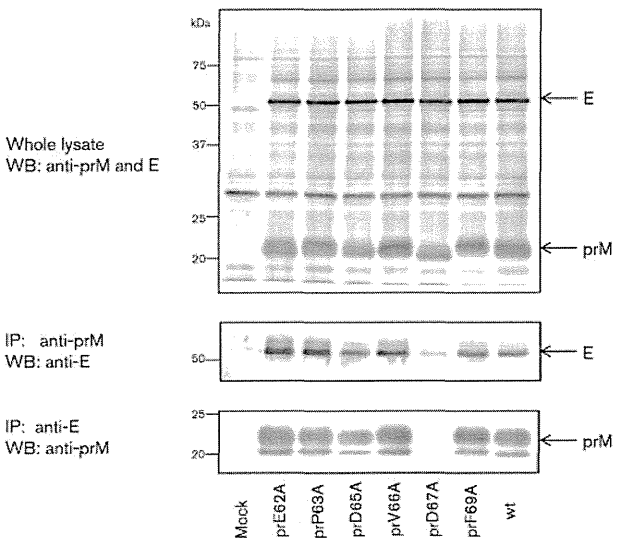

Fig. 2. Effect of mutations in the conserved region of prM on prM–E interaction. The prM protein, with or without (wt) a mutation in the conserved region, was expressed in 293T cells by transfection of the pCAG-TBEME plasmid containing various mutations. After 24 h incubation, cells were harvested, and whole-cell lysate and post-nuclear supernatant immunoprecipitated (IP) with mouse anti-E or anti-prM antibodies were analysed by Western blotting (WB). Protein bands were detected by anti-E and anti-prM rabbit polyclonal antibodies. The positions of the individual proteins are marked and molecular size is indicated (kDa).

and assembly of SPs were engineered in the full-length infectious cDNA of TBEV (Oshima-IC) (Table 2). Baby hamster kidney (BHK-21) cells were transfected with *in vitro*-transcribed mRNA from Oshima-IC, and the culture supernatant was harvested at 8–120 h post-transfection. As presented in Fig. 5(a), cells transfected with Oshima-IC containing prM mutations produced fewer infectious virus particles than cells transfected with wild-type Oshima-IC. The secreted E protein was quantified by ELISA and compared with the infectious virus titre to examine whether the lower level of infectious virus resulting from the presence of prM mutations was due to a reduction in virion secretion or to loss of infectivity of the secreted virion (Fig. 5b). Virus titres were reduced by the prM mutations at a rate similar to that of viral protein secretion, indicating that the infectivity of secreted virions was unaffected by the prM mutations. These results were consistent with the low level of secretion of SPs by prM mutations observed in Fig. 1. Cells transfected with Oshima-IC prD67A produced fewer virus particles than those transfected with Oshima-IC containing the other prM mutations, indicating that this mutation affects the virus multiplication associated with the loss of the prM–E interaction and particle assembly, as observed in the SP experiment.

To investigate the possibility of the appearance of reversion or second-site mutations, each virus was passaged ten times (over a period of 30 days) and the nucleotide sequences of their prM and E genes were determined. Reversion to wild-type sequence was observed in Oshima-IC prP63A at passage 9 and in prD67A at passage 2. No reversion or second-site mutation appeared in Oshima-IC prD65A, prV66A or prF69A, and their growth rates were still slower than wild-type virus. These data confirmed the importance of the conserved region in prM in viral multiplication.

Molecular modelling of the conserved region on trimeric spikes of immature virions

To identify potential amino acid residues that could interact with the conserved regions, the crystal structure of the pr peptide and the E protein was superimposed on the pseudo-atomic structure of the trimeric spikes of three prM–E heterodimers in immature virions. This structure was then refined by simulated annealing with molecular dynamics calculation (Fig. 6 and Supplementary Table S1, available in JGV Online). This highlighted amino acid residues that could potentially interact with the conserved regions of the prM proteins (prM-1, prM-2 and prM-3) within the trimeric spike of the prM–E heterodimers: (i) the fusion peptide of E-2 with the conserved region of prM-1; (ii) arginine-16, lysine-19, methionine-39 and threonine-81 of prM-3 with the conserved region of prM-2; and (iii) arginine-16, lysine-19, methionine-39 and threonine-81 of prM-2 with the conserved region of prM-3. As shown in Fig. 6, whilst the conserved region of prM-1 is located between the fusion loop of E-1 and E-2, the conserved regions of prM-2 and prM-3 were suggested to interact with similar regions of each other, indicating the dimeric association between prM-2 and prM-3. These results suggest that the conserved region in prM could serve as an important domain for the association between heterodimers in the formation of a spike.

DISCUSSION

In flaviviruses, the prM and E proteins play important roles in the assembly and secretion of virions. Many studies have demonstrated that the co-expression of prM and E proteins in cells leads to the formation of SPs that are structurally and functionally similar to native virions (Allison *et al.*, 1995b; Fonseca *et al.*, 1994; Mason *et al.*, 1991; Op De Beeck *et al.*, 2003; Yamshchikov & Compans, 1993). These studies indicated that critical determinants for the assembly and secretion of the virions were present in the prM and/or E proteins. During the assembly process, prM proteins are assumed to coat E proteins. It has been shown that the furin cleavage sequence between the pr region and the M protein is important for maturation of infectious virions prior to their release from cells (Elshuber *et al.*, 2003; Stadler *et al.*, 1997) and that the transmembrane domain of the prM protein serves as a retention signal for the membrane of the ER (Op De Beeck *et al.*, 2003, 2004). In several reports, single point mutations in prM were found

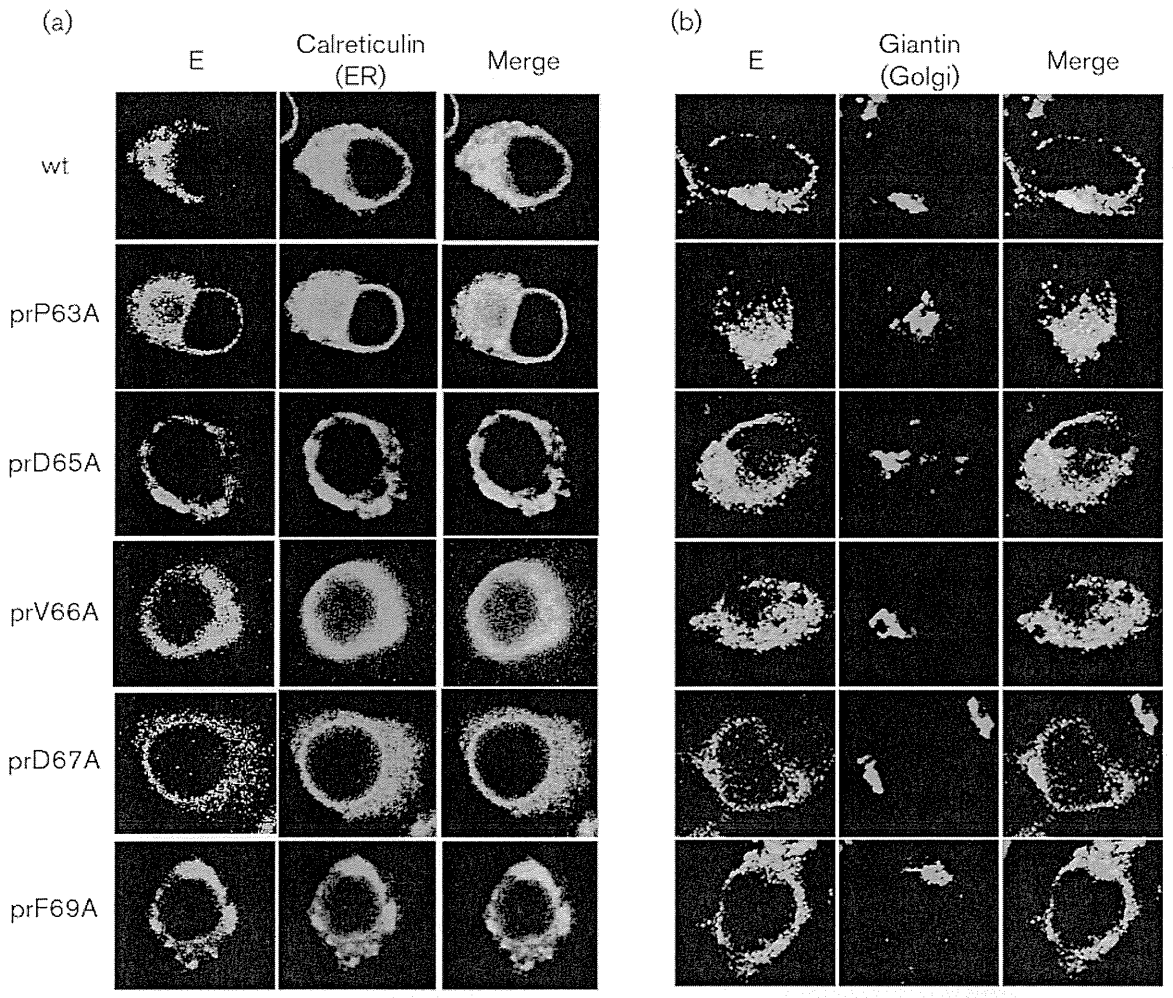

Fig. 3. Intracellular localization of expressed E proteins. 293T cells transfected with pCAG-TBEME wild-type (wt) or various mutant plasmids were fixed and subjected to dual staining with antibodies against calreticulin (an ER marker) (a) or giantin (a Golgi marker) (b) and anti-E antibodies. Co-localization of the E protein with the ER or Golgi marker proteins is depicted in the merged images.

to affect viral particle formation and secretion without preventing prM–E heterodimerization (Pryor *et al.*, 2004; Tan *et al.*, 2009). Another study showed that coordinated cleavage between the C protein and prM promoted the uptake of nucleocapsids into budding flavivirus membranes (Lobigs & Lee, 2004). However, little is known about the functional residues of the prM protein involved in the assembly and secretion process. In this study, we demonstrated for the first time that the conserved region of the prM ectodomain in flaviviruses has critical functions in the assembly and secretion process.

Multiple-sequence analysis revealed that the conserved region in prM is present in a large number of flaviviruses, including tick-borne, mosquito-borne and no-known-vector flaviviruses (Table 1). As shown in our previous study, a proline-to-serine mutation at position 63 of the prM of TBEV reduces the secretion of virus particles (Yoshii *et al.*, 2004) and we considered that the conserved region plays a crucial role in the assembly and secretion of virus particles. It was revealed that the secretion of SPs was impaired by a single mutation in the conserved region of both TBEV and JEV (Fig. 1). This indicated that the conserved region in the prM protein is a critical and common molecular determinant for the assembly and secretion of flaviviruses.

The interaction between the prM and E proteins is important during the early events of virus particle maturation and assembly. Previous studies have shown that the E protein requires co-synthesis of prM to achieve structural conformation, whilst prM folds independently of other viral components (Guirakhoo *et al.*, 1992; Lorenz *et al.*, 2002). PrM–E heterodimerization is a crucial process

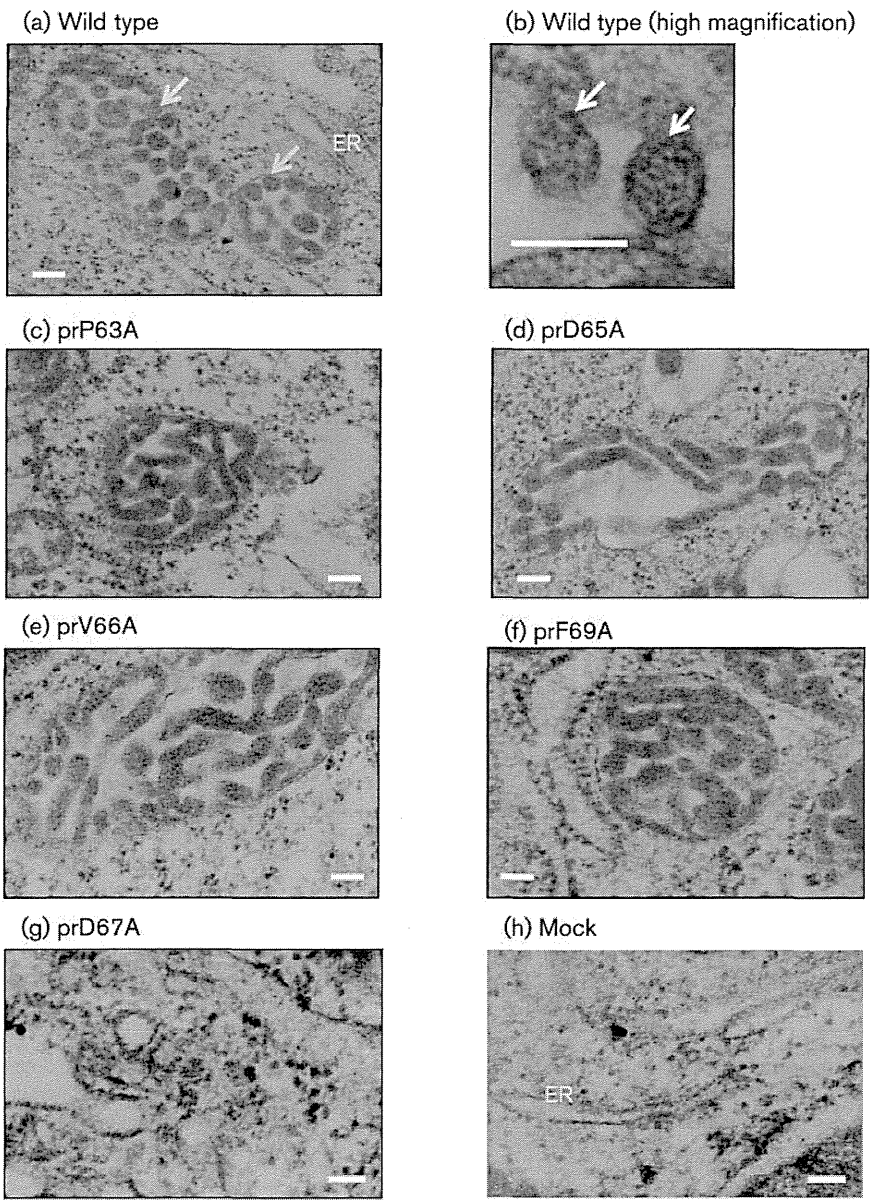

Fig. 4. Electron micrographs of 293T cells transfected with pCAG-TBEME containing various mutations. (a, b) Spherical SPs (arrows; diameter 20–30 nm) were observed in the lumen of membrane-bound vesicles in wild-type-transfected cells. (c–f) Filamentous structures were observed in the lumen of membrane-bound vesicles in cells transfected with pCAG-TBEME containing the prP63A (c), prD65A (d), prV66A (e) or prF69A (f) mutation. (g, h) No particulate and filamentous structures were observed in prD67A-transfected cells (g), similar to mock-transfected control cells (h). Bars, 50 nm.

for sequential virus particle formation. In this study, co-immunoprecipitation experiments demonstrated that prM–E heterodimerization was not impaired by the mutations in the conserved region of the prM protein except for the mutation at position 67 (Fig. 2). This mutation impaired the interaction between the prM and E protein, leading to the failure of further steps in the viral particle assembly process. These data suggested that the reduction in SP secretion by the prM mutations, except for position 67, was due to later steps in the viral particle assembly process and secretion, and not to disruption of prM–E heterodimerization in the early events of virus particle assembly.

Previous reports have shown that flavivirus particles bud into the ER lumen, followed by transport through the

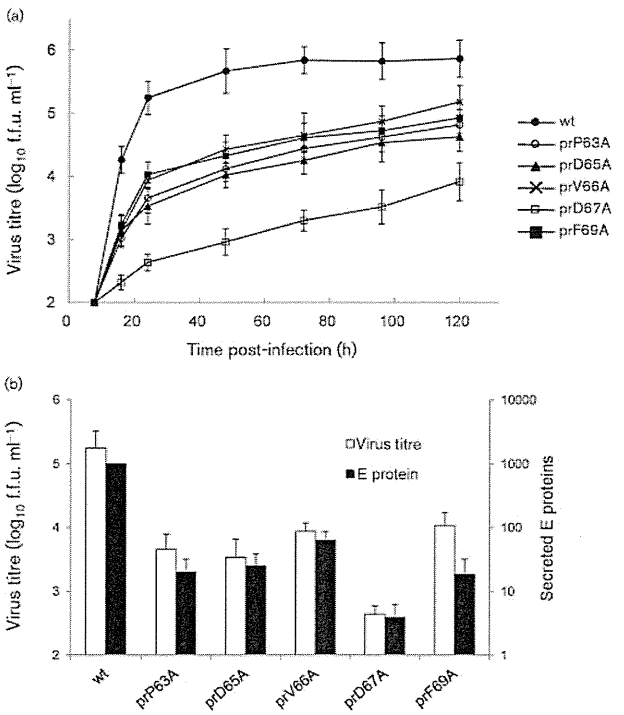

Fig. 5. Effect of mutations in the conserved region of prM on virus particle secretion. (a) Growth curve of the Oshima-IC virus wild-type (wt) and prP63A, prD65A, prV66A, prD67A and prF69A mutants. A monolayer of BHK-21 cells was infected with the individual viruses at an m.o.i. of 0.01. At each time point, the culture medium was harvested and virus titres were determined by focus-forming assay in BHK cells. (b) Comparison of the titre of infectious virus and secreted E proteins. After 24 h incubation, the relative amount of secreted E protein was quantified by ELISA and compared with the virus titre. The amount of E protein from the Oshima-IC wild-type virus was set at 1000. Data are means ± SD from triplicate experiments.

secretory pathway (Mackenzie & Westaway, 2001). In this study, the expressed viral proteins with the prM mutations were not transported to the Golgi complex, and accumulated in the ER (Fig. 3). Furthermore, ultrastructural analysis revealed long filamentous structures, rather than spherical SPs, in the lumen of the ER resulting from the prM mutations (Fig. 4). The width of the filamentous structures was approximately the same as the diameter of the SPs, and constrictions were observed every 50–100 nm. It was suggested that they were derived from abnormal budding in which a particle failed to pinch off, resulting in the bud growing into a tubular structure. Filamentous structures may not undergo transport through the secretory pathway due to their abnormal budding. It is also possible that they are derived from cellular membrane components induced by prM mutations. In any case, the mutations in the conserved region of prM clearly affected the budding process of the virus particle, which must have occurred after the prM–E heterodimerization. No SPs or filamentous structures were observed with the mutation at position 67. This could be attributed to the disruption or the prM–E heterodimerization in the early events of virus particle assembly, as described above. In a study of dengue virus, this negatively charged residue was shown to interact with the positively charged surface of domain II of the E protein (Li *et al.*, 2008).

The budding mechanism of flaviviruses is considered to be distinct from that of other enveloped viruses. In many enveloped viruses, important cytoplasmic domains directing virus budding have been identified, such as late-domain motifs (Bieniasz, 2006; Kail *et al.*, 1991; Morita & Sundquist, 2004; Whitt *et al.*, 1989; Zhao *et al.*, 1994). These domains interact with cellular factors resulting in efficient budding. However, the cytoplasmic loops of the flavivirus prM and E proteins consist of only a few amino acid residues between their two transmembrane regions. Thus, it is considered that the ER-luminal regions of the prM and/or E proteins play critical roles in the assembly of flaviviruses. The ER membrane does not normally form vesicles that bud into the lumen. It is possible that prM–E heterodimers, alone or with cellular factors in the ER lumen, assemble laterally and induce membrane curvature into an isometric lattice, as reported in the budding of membrane transport vesicles (Keen *et al.*, 1979; Wieland & Harter, 1999). The conserved region in prM may have important roles in this process, which were impaired by the mutations, leading to the abnormal budding.

The conserved region in prM could be involved in the oligomerization of the prM–E heterodimers. Immature virions of flaviviruses contain 60 trimeric spikes and each spike consists of three prM–E heterodimers (Zhang *et al.*, 2003). The asymmetrical spike has been considered a single assembly unit because the association between heterodimers within a spike is sufficiently strong, compared with the association between spikes. The dominant contacts between the prM–E heterodimers within a spike are between pre-peptides at the extremities of the spikes. Based on the crystal structure of the pr peptide of dengue virus 2 (Li *et al.*, 2008), the conserved region of prM covers the fusion peptide of the E protein in each heterodimer and aspartate-63 and -65 were involved in the complementary electrostatic patches. Our structural model for an asymmetrical trimer of prM–E heterodimers indicates that the conserved region in prM could serve as an important domain for the association between heterodimers in the formation of a spike (Fig. 6 and Supplementary Table S1). The mutations in the region might affect the association between heterodimers and cause perturbation of oligomerization of prM–E heterodimers, resulting in the inefficient induction of membrane curvature and/or pinch-off.

In summary, we demonstrated that the conserved region in prM is a critical determinant in flavivirus assembly and secretion. Mutations in this region, except for aspartate-67,

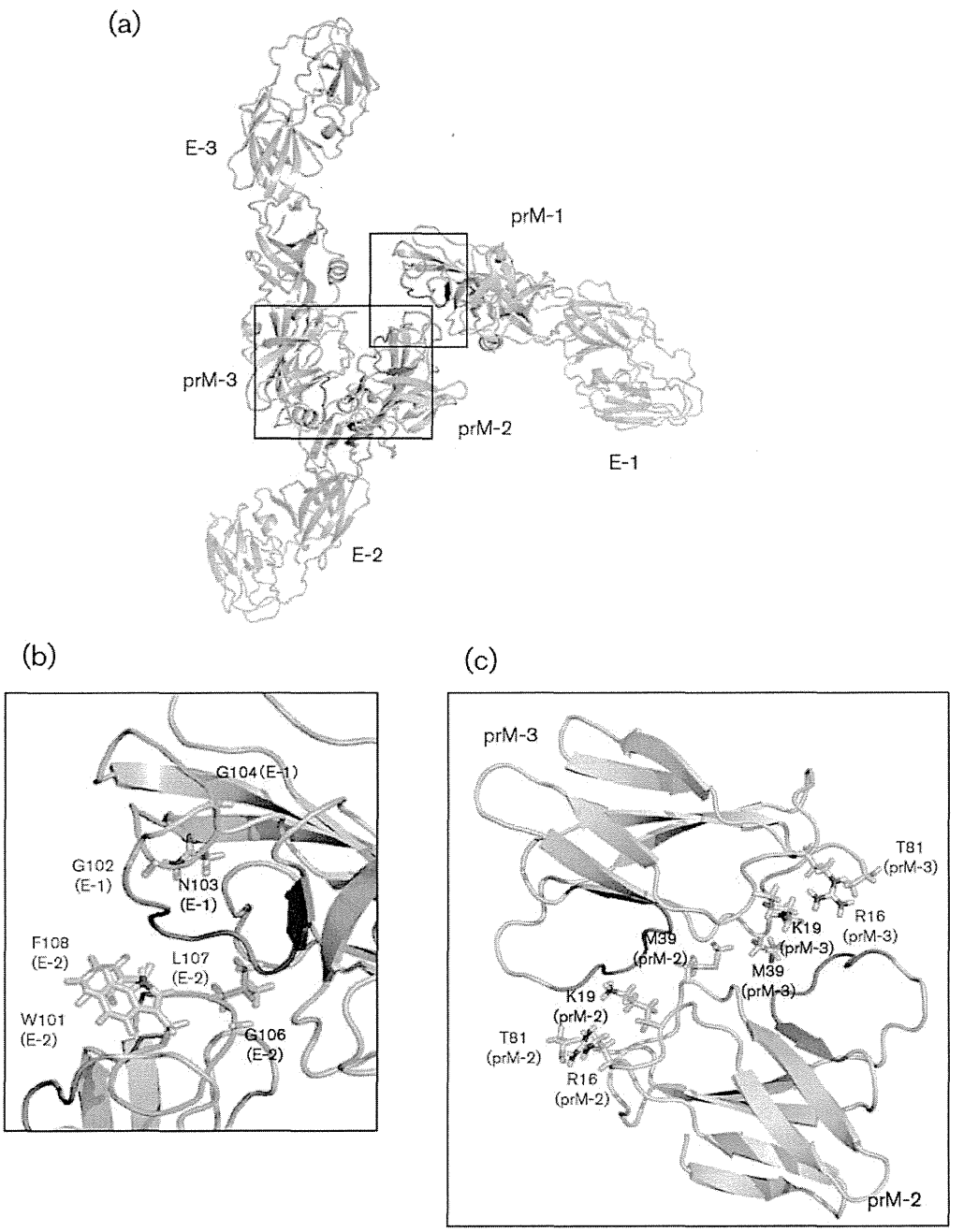

Fig. 6. Structural model for an asymmetrical trimer of prM–E heterodimers. (a) Overall structure of an asymmetrical trimer of prM–E heterodimers. (b) Close-up view of the binding interface between prM-1 and E-1 or E-2. (c) Close-up view of the binding interface between prM-2 and prM-3. E and prM molecules are coloured blue-white and yellow, respectively. The fusion peptide of the E protein and the conserved region of prM protein are shown in green and magenta, respectively. Residues represented by stick models show the amino acid position within 4.0 Å of the conserved region of prM. This figure was prepared using PyMOL (DeLano Scientific; DeLano, 2002).

did not affect the interaction between the prM and E proteins but impaired the budding step, which is independent of previously known functions of the prM protein. These results contribute to the further understanding of prM function, revealing the molecular mechanism of flavivirus assembly and secretion.

METHODS

Cells. BHK-21 cells were grown at 37 °C in minimum essential medium supplemented with 8 % (v/v) FCS and L-glutamine. Human embryonic kidney 293T cells were cultured at 37 °C in Dulbecco's modified Eagle's medium, containing 10 % (v/v) FCS, L-glutamine and penicillin/streptomycin.

Antibodies. For the detection of TBEV prM and E proteins by ELISA, immunoprecipitation and immunofluorescence experiments, mouse anti-E mAbs 1H4 and 4H8, prepared in our laboratory, were used (Komoro *et al.*, 2000). Rabbit polyclonal anti-prM and anti-E antibodies were prepared by immunization with recombinant prM and E proteins, as described previously (Yoshii *et al.*, 2004). Mouse anti-E mAb 10B4 was kindly provided by Dr Konishi (Kobe University Graduate School of Medicine, Kobe, Japan) for the detection of JEV E protein by Western blotting. For the immunofluorescence co-localization studies, anti-calreticulin rabbit polyclonal antiserum (Affinity BioReagents) or anti-giantin rabbit polyclonal antiserum (Covance Research Products) was used. FITC-conjugated anti-mouse IgG antibodies and Texas Red-conjugated anti-rabbit IgG antibodies (Jackson Immunoresearch) were used as secondary antibodies in the immunofluorescence assays, and alkaline phosphatase-conjugated anti-rabbit and anti-mouse IgG antibodies (Jackson Immunoresearch) were used in the Western blot analysis.

Plasmids. Plasmid pCAG-TBEME, a pCAGGS-based plasmid encoding the TBEV (Oshima 5-10 strain) signal sequence of the prM, and the prM and E genes, was constructed as described previously (Yoshii *et al.*, 2003).

Plasmid pcJEME, a pcDNA3-based plasmid that encodes the JEV (Nakayama strain) signal sequence of prM, and the prM and E genes, was kindly provided by Dr Konishi and by Dr Mason (Department of Pathology, University of Texas Medical Branch, Galveston, TX, USA) (Konishi *et al.*, 1998),

The TBEV infectious cDNA clone used, Oshima-IC, was constructed previously (Hayasaka *et al.*, 2004).

All mutations within the conserved sequence of the prM protein were engineered in the pCAG-TBEME, pcJEME and Oshima-IC full-length plasmid constructs using standard PCR mutagenesis techniques (Table 2).

Expression of viral prM and E proteins. 293T cells were transfected with each plasmid complexed to *Trans*IT-LT1 reagent (PanVera) in Opti-MEM (Invitrogen), as described previously (Yoshii *et al.*, 2003). After a 24 h incubation, the cells and supernatant were harvested and used for further experiments.

ELISA. The E protein of TBEV was detected by ELISA, as described previously (Yoshii *et al.*, 2003). Briefly, transfected cells were lysed with 1 % (v/v) Triton X-100 in 10 mM Tris-buffered saline (TBS) and the supernatants were treated with 1 % Triton X-100. Triton X-100-solubilized samples were added to mAb 1H4-coated wells of 96-well microtitre ELISA plates, previously blocked with 3 % (w/v) BSA. The E protein was detected by incubation with biotinylated mAb 4H8 and HRP-conjugated streptavidin (Sigma). HRP activity was detected by adding *o*-phenylenediamine dihydrochloride (Sigma) in the presence of 0.03 % (v/v) H_2O_2 and absorbance was measured at 450–620 nm.

Immunoprecipitation. 293T cells were transfected with pCAG-TBEME containing the various mutations, as described above. After a 24 h incubation, the cells were lysed with Triton X-100 in 10 mM TBS, incubated on ice for 20 min and centrifuged (16 000 *g*, 20 min). The supernatant, which excluded the nuclear fraction, was pre-cleared on protein G–Sepharose beads (Amersham Pharmacia Biotech) for 2 h at 4 °C. Pre-cleared lysates were combined with protein G–Sepharose beads with mAb 1H4 and precipitated by incubation for 2 h at 4 °C. Immune complexes were pelleted (10 000 *g*, 10 s) and washed four times with 1 % Triton X-100 in 10 mM TBS. Subsequently, the precipitated materials were solubilized and analysed by SDS-PAGE and Western blotting.

SDS-PAGE and Western blotting. Protein samples were separated by SDS-PAGE [12 % (w/v) acrylamide]. The protein bands were transferred onto PVDF membranes and incubated with 1 % (w/v) gelatin in 25 mM TBS containing 0.01 % (v/v) Tween 20 (TBST). After washing with TBST, the membranes were reacted with an antibody against the viral protein of TBEV or JEV, followed by alkaline phosphatase-conjugated secondary antibody. Protein bands were visualized using an alkaline phosphatase detection reagent kit (Novagen), according to the manufacturer's protocol.

Immunofluorescence assay. 293T cells were grown on eight-well chamber slides (Nalge Nunc International) and transfected with pCAG-TBEME containing the various mutations. After 8 h incubation, cells were rinsed with PBS, fixed with 4 % (w/v) paraformaldehyde for 10 min and permeabilized with 0.2 % (v/v) Triton X-100 for 4 min at room temperature. After blocking with 2 % (w/v) BSA, the cells were incubated for 1 h with mouse mAb 1H4 and antibodies that recognize marker proteins of various cellular organelles or anti-prM antibody. After extensive washing, the cells were incubated with fluorescently labelled conjugated secondary antibodies. The cells were washed three times with PBS, followed by mounting of the coverslips on glass slides. Images were viewed and collected with an Olympus IX70 confocal microscope.

Electron microscopy. 293T cells were transfected with pCAG-TBEME containing the various mutations. After a 24 h incubation, the cells were harvested and centrifuged (1000 *g*, 5 min). The pellets were fixed with 3 % (v/v) glutaraldehyde in 0.1 M phosphate buffer (pH 7.2) for 3 h and rinsed three times with 0.1 M phosphate buffer. After post-fixation in a 1 % (w/v) osmium tetroxide solution for 1.5 h, the pellets were dehydrated through a series of graded ethanols and embedded in Epon 812 via QY1 (Nishin EM). Ultrathin sections were cut, stained with uranyl acetate and lead citrate, and examined under a JEM 1210 transmission electron microscope (JEOL) at an acceleration voltage of 80 kV.

Virus recovery and titration. Infectious RNA was transcribed from the Oshima-IC plasmid using an mMESSAGE mMACHINE SP6 kit (Ambion) and electroporated into BHK-21 cells, as described previously (Hayasaka *et al.*, 2004). At 1–5 days post-electroporation, the secreted virus was recovered and the infectious virus titre was assayed using a focus count assay, as described previously (Takashima *et al.*, 1997). Briefly, monolayers of BHK-21 cells were grown in 96-well plates and inoculated with serial dilutions of the virus. After 38 h incubation, virus foci were visualized by immunofluorescent staining using anti-TBEV E antibodies.

Passaging experiments. Passages of the virus on BHK-21 cells were performed by transferring aliquots (200 µl) of cell culture supernatants (at 3 days post-infection) cleared of cell debris and insoluble material by low-speed centrifugation to fresh BHK-21 cells grown in 24-well culture plates.

Molecular modelling. The model structure for an asymmetrical trimer of prM–E heterodimers was generated by superimposing the crystal structure of dengue 2 virus (Protein Data Bank code: 3C6E) onto the pseudo-atomic structure determined by cryo-electron microscopy (Protein Data Bank code: 3C6D). This structure was refined by molecular dynamics simulations followed by energy minimizations. First, the system was gradually heated from 50 to

1000 K for 13 ps of simulation and then cooled to 300 K for 10 ps. A harmonic constraint of 10 kcal mol^{-1} $Å^{-2}$ was applied on the Cα atoms of the protein during the simulation. The time step was set to 1 fs. After molecular dynamics simulations, the energy minimization was conducted without positional constraints using 10 000 steps of steepest descent, followed by conjugate gradient minimization, until the root mean square gradient was $\leqslant 0.01$ kcal mol^{-1} $^{-}Å$. All molecular dynamics and energy minimization calculations were performed using Discovery Studio 2.5 (Accelrys, http://accelrys.com/products/discovery-studio/) with a CHARMm force field with a generalized Born implicit solvent model.

ACKNOWLEDGEMENTS

We thank Dr Konishi and Dr Mason for providing the pcJEME plasmid and anti-JEV mAbs. This work was supported by Grants-in-Aid for Scientific Research (22780268) and the Global COE Program from the Ministry of Education, Culture, Sports, Sciences and Technology of Japan, and Health Sciences Grants for Research on Emerging and Re-emerging Infectious Disease from the Ministry of Health, Labour and Welfare of Japan.

REFERENCES

Allison, S. L., Schalich, J., Stiasny, K., Mandl, C. W., Kunz, C. & Heinz, F. X. (1995a). Oligomeric rearrangement of tick-borne encephalitis virus envelope proteins induced by an acidic pH. *J Virol* **69**, 695–700.

Allison, S. L., Stadler, K., Mandl, C. W., Kunz, C. & Heinz, F. X. (1995b). Synthesis and secretion of recombinant tick-borne encephalitis virus protein E in soluble and particulate form. *J Virol* **69**, 5816–5820.

Allison, S. L., Stiasny, K., Stadler, K., Mandl, C. W. & Heinz, F. X. (1999). Mapping of functional elements in the stem-anchor region of tick-borne encephalitis virus envelope protein E. *J Virol* **73**, 5605–5612.

Allison, S. L., Schalich, J., Stiasny, K., Mandl, C. W. & Heinz, F. X. (2001). Mutational evidence for an internal fusion peptide in flavivirus envelope protein E. *J Virol* **75**, 4268–4275.

Bieniasz, P. D. (2006). Late budding domains and host proteins in enveloped virus release. *Virology* **344**, 55–63.

Chambers, T. J., Hahn, C. S., Galler, R. & Rice, C. M. (1990). Flavivirus genome organization, expression, and replication. *Annu Rev Microbiol* **44**, 649–688.

DeLano, W. L. (2002). *The PyMol Molecular Graphics System.* San Carlos, CA: DeLano Scientific.

Elshuber, S., Allison, S. L., Heinz, F. X. & Mandl, C. W. (2003). Cleavage of protein prM is necessary for infection of BHK-21 cells by tick-borne encephalitis virus. *J Gen Virol* **84**, 183–191.

Finn, R. D., Mistry, J., Tate, J., Coggill, P., Heger, A., Pollington, J. E., Gavin, O. L., Gunasekaran, P., Ceric, G. & other authors (2010). The Pfam protein families database. *Nucleic Acids Res* **38** (Database issue), D211–D222.

Fonseca, B. A., Pincus, S., Shope, R. E., Paoletti, E. & Mason, P. W. (1994). Recombinant vaccinia viruses co-expressing dengue-1 glycoproteins prM and E induce neutralizing antibodies in mice. *Vaccine* **12**, 279–285.

Gritsun, T. S., Lisak, V. M., Liapustin, V. N., Korolev, M. B. & Lashkevich, V. A. (1989). [Slowly-sedimenting hemagglutinin of the tick-borne encephalitis virus]. *Vopr Virusol* **34**, 449–454 (in Russian).

Guirakhoo, F., Heinz, F. X., Mandl, C. W., Holzmann, H. & Kunz, C. (1991). Fusion activity of flaviviruses: comparison of mature and immature (prM-containing) tick-borne encephalitis virions. *J Gen Virol* **72**, 1323–1329.

Guirakhoo, F., Bolin, R. A. & Roehrig, J. T. (1992). The Murray Valley encephalitis virus prM protein confers acid resistance to virus particles and alters the expression of epitopes within the R2 domain of E glycoprotein. *Virology* **191**, 921–931.

Hayasaka, D., Gritsun, T. S., Yoshii, K., Ueki, T., Goto, A., Mizutani, T., Kariwa, H., Iwasaki, T., Gould, E. A. & Takashima, I. (2004). Amino acid changes responsible for attenuation of virus neurovirulence in an infectious cDNA clone of the Oshima strain of tick-borne encephalitis virus. *J Gen Virol* **85**, 1007–1018.

Heinz, F. & Kunz, C. (1977). Concentration and purification of tick-borne encephalitis virus grown in suspensions of chick embryo cells. *Acta Virol* **21**, 301–307.

Heinz, F. X., Stiasny, K., Püschner-Auer, G., Holzmann, H., Allison, S. L., Mandl, C. W. & Kunz, C. (1994). Structural changes and functional control of the tick-borne encephalitis virus glycoprotein E by the heterodimeric association with protein prM. *Virology* **198**, 109–117.

Kail, M., Hollinshead, M., Ansorge, W., Pepperkok, R., Frank, R., Griffiths, G. & Vaux, D. (1991). The cytoplasmic domain of alphavirus E2 glycoprotein contains a short linear recognition signal required for viral budding. *EMBO J* **10**, 2343–2351.

Keen, J. H., Willingham, M. C. & Pastan, I. H. (1979). Clathrin-coated vesicles: isolation, dissociation and factor-dependent reassociation of clathrin baskets. *Cell* **16**, 303–312.

Komoro, K., Hayasaka, D., Mizutani, T., Kariwa, H. & Takashima, I. (2000). Characterization of monoclonal antibodies against Hokkaido strain tick-borne encephalitis virus. *Microbiol Immunol* **44**, 533–536.

Konishi, E. & Mason, P. W. (1993). Proper maturation of the Japanese encephalitis virus envelope glycoprotein requires cosynthesis with the premembrane protein. *J Virol* **67**, 1672–1675.

Konishi, E., Yamaoka, M., Khin-Sane-Win, Kurane, I. & Mason, P. W. (1998). Induction of protective immunity against Japanese encephalitis in mice by immunization with a plasmid encoding Japanese encephalitis virus premembrane and envelope genes. *J Virol* **72**, 4925–4930.

Kuhn, R. J., Zhang, W., Rossmann, M. G., Pletnev, S. V., Corver, J., Lenches, E., Jones, C. T., Mukhopadhyay, S., Chipman, P. R. & Strauss, E. G. (2002). Structure of dengue virus: implications for flavivirus organization, maturation, and fusion. *Cell* **108**, 717–725.

Li, L., Lok, S. M., Yu, I. M., Zhang, Y., Kuhn, R. J., Chen, J. & Rossmann, M. G. (2008). The flavivirus precursor membrane–envelope protein complex: structure and maturation. *Science* **319**, 1830–1834.

Lindenbach, B. D., Thiel, H. J. & Rice, C. M. (2007). *Flaviviridae:* the viruses and their replication. In *Fields Virology*, 5th edn, pp. 1101–1152. Edited by D. M. Knipe & P. M. Howley. Philadelphia: Lippincott Williams & Wilkins.

Lobigs, M. & Lee, E. (2004). Inefficient signalase cleavage promotes efficient nucleocapsid incorporation into budding flavivirus membranes. *J Virol* **78**, 178–186.

Lorenz, I. C., Allison, S. L., Heinz, F. X. & Helenius, A. (2002). Folding and dimerization of tick-borne encephalitis virus envelope proteins prM and E in the endoplasmic reticulum. *J Virol* **76**, 5480–5491.

Lorenz, I. C., Kartenbeck, J., Mezzacasa, A., Allison, S. L., Heinz, F. X. & Helenius, A. (2003). Intracellular assembly and secretion of recombinant subviral particles from tick-borne encephalitis virus. *J Virol* **77**, 4370–4382.

Mackenzie, J. M. & Westaway, E. G. (2001). Assembly and maturation of the flavivirus Kunjin virus appear to occur in the rough endoplasmic reticulum and along the secretory pathway, respectively. *J Virol* **75**, 10787–10799.

Mason, P. W., Pincus, S., Fournier, M. J., Mason, T. L., Shope, R. E. & Paoletti, E. (1991). Japanese encephalitis virus–vaccinia recombinants produce particulate forms of the structural membrane proteins and induce high levels of protection against lethal JEV infection. *Virology* **180**, 294–305.

Morita, E. & Sundquist, W. I. (2004). Retrovirus budding. *Annu Rev Cell Dev Biol* **20**, 395–425.

Op De Beeck, A., Molenkamp, R., Caron, M., Ben Younes, A., Bredenbeek, P. & Dubuisson, J. (2003). Role of the transmembrane domains of prM and E proteins in the formation of yellow fever virus envelope. *J Virol* **77**, 813–820.

Op De Beeck, A., Rouillé, Y., Caron, M., Duvet, S. & Dubuisson, J. (2004). The transmembrane domains of the prM and E proteins of yellow fever virus are endoplasmic reticulum localization signals. *J Virol* **78**, 12591–12602.

Pryor, M. J., Azzola, L., Wright, P. J. & Davidson, A. D. (2004). Histidine 39 in the dengue virus type 2 M protein has an important role in virus assembly. *J Gen Virol* **85**, 3627–3636.

Stadler, K., Allison, S. L., Schalich, J. & Heinz, F. X. (1997). Proteolytic activation of tick-borne encephalitis virus by furin. *J Virol* **71**, 8475–8481.

Takashima, I., Morita, K., Chiba, M., Hayasaka, D., Sato, T., Takezawa, C., Igarashi, A., Kariwa, H., Yoshimatsu, K. & other authors (1997). A case of tick-borne encephalitis in Japan and isolation of the virus. *J Clin Microbiol* **35**, 1943–1947.

Tan, T. T., Bhuvanakantham, R., Li, J., Howe, J. & Ng, M. L. (2009). Tyrosine 78 of premembrane protein is essential for assembly of West Nile virus. *J Gen Virol* **90**, 1081–1092.

Wengler, G. & Wengler, G. (1989). Cell-associated West Nile flavivirus is covered with E + pre-M protein heterodimers which are destroyed and reorganized by proteolytic cleavage during virus release. *J Virol* **63**, 2521–2526.

Whitt, M. A., Chong, L. & Rose, J. K. (1989). Glycoprotein cytoplasmic domain sequences required for rescue of a vesicular stomatitis virus glycoprotein mutant. *J Virol* **63**, 3569–3578.

Wieland, F. & Harter, C. (1999). Mechanisms of vesicle formation: insights from the COP system. *Curr Opin Cell Biol* **11**, 440–446.

Yamshchikov, V. F. & Compans, R. W. (1993). Regulation of the late events in flavivirus protein processing and maturation. *Virology* **192**, 38–51.

Yoshii, K., Hayasaka, D., Goto, A., Obara, M., Araki, K., Yoshimatsu, K., Arikawa, J., Ivanov, L., Mizutani, T. & other authors (2003). Enzyme-linked immunosorbent assay using recombinant antigens expressed in mammalian cells for serodiagnosis of tick-borne encephalitis. *J Virol Methods* **108**, 171–179.

Yoshii, K., Konno, A., Goto, A., Nio, J., Obara, M., Ueki, T., Hayasaka, D., Mizutani, T., Kariwa, H. & Takashima, I. (2004). Single point mutation in tick-borne encephalitis virus prM protein induces a reduction of virus particle secretion. *J Gen Virol* **85**, 3049–3058.

Zhang, Y., Corver, J., Chipman, P. R., Zhang, W., Pletnev, S. V., Sedlak, D., Baker, T. S., Strauss, J. H., Kuhn, R. J. & Rossmann, M. G. (2003). Structures of immature flavivirus particles. *EMBO J* **22**, 2604–2613.

Zhao, H., Lindqvist, B., Garoff, H., von Bonsdorff, C. H. & Liljeström, P. (1994). A tyrosine-based motif in the cytoplasmic domain of the alphavirus envelope protein is essential for budding. *EMBO J* **13**, 4204–4211.

Am. J. Trop. Med. Hyg., 86(3), 2012, pp. 545–553
doi:10.4269/ajtmh.2012.11-0297

Isolation and Characterization of Hantaviruses in Far East Russia and Etiology of Hemorrhagic Fever with Renal Syndrome in the Region

Hiroaki Kariwa,* Keisuke Yoshikawa, Yoichi Tanikawa, Takahiro Seto, Takahiro Sanada, Ngonda Saasa, Leonid I. Ivanov, Raisa Slonova, Tatyana A. Zakharycheva, Ichiro Nakamura, Kumiko Yoshimatsu, Jiro Arikawa, Kentaro Yoshii, and Ikuo Takashima

Graduate School of Veterinary Medicine, Hokkaido University, Sapporo, Japan; Plague Control Station of Khabarovsk, Khabarovsk, Russia; Research Institute of Epidemiology and Microbiology, Siberian Branch of Russian Academy of Medical Sciences, Vladivostok, Russia; Far Eastern State Medical University, Khabarovsk, Russia; Research Center for Zoonosis Control, Hokkaido University, Sapporo, Japan; Graduate School of Medicine, Hokkaido University, Sapporo, Japan

Abstract. Hemorrhagic fever with renal syndrome (HFRS) is a serious public health issue in Far East Russia. Two different hantaviruses were isolated from rodents captured in the Khabarovsk region: Amur virus (AMRV; Khekhtsir/AP209/2005 strain from *Apodemus peninsulae*) and Hantaan virus (HTNV; Galkino/AA57/2002 strain from *A. agrarius*). Genetic analysis of the new isolates revealed that the M and L segments were apparently different between AMRV and HTNV, but S segments of the two viruses were closer. The antigenicities of AMRV, HTNV, and Seoul virus (SEOV) were differentiated by cross-neutralization. Serological differential diagnoses of 67 HFRS patients in the Prymorsky and Khabarovsk regions of Far East Russia were conducted using a neutralization test. The results revealed that the major cause of HFRS varied with location in Far East Russia: SEOV for Vladivostok city in the Prymorsky region, AMRV in rural areas of the Primorsky region, and probably HTNV for the Khabarovsk region.

INTRODUCTION

Hantaviruses are the causative agents of hemorrhagic fever with renal syndrome (HFRS) and hantavirus pulmonary syndrome (HPS) in humans.[1,2] Rodents and *Soricomorpha* species are natural reservoirs of these viruses, and humans acquire infection by inhaling the excreta of infected animals. Hantaviruses are classified in the genus *Hantavirus* within the family *Bunyaviridae*, and they possess a genome composed of three negative-stranded RNA segments. The small (S), medium (M), and large (L) genome segments encode nucleocapsid protein (N), two glycoproteins (Gn and Gc), and RNA polymerase, respectively.[3] Each rodent-borne hantavirus has its own host, and more than 40 species of hantaviruses have been identified.[4,5] Some rodent-borne hantaviruses cause HFRS or HPS and are considered to be important zoonotic agents in various countries around the world.

About 20,000–50,000 cases of HFRS are reported annually worldwide, and large proportions of the infections are from the East Eurasian continent, including China, Korea, and Far East Russia.[6–8] Hantaan virus (HTNV) and Seoul virus (SEOV) are known to cause severe and mild forms of HFRS in the Eastern Eurasian Continent, respectively.[2,9,10] HTNV is carried by the striped field mouse, *Apodemus agrarius*, which preferentially inhabits grass and rice fields. Thus, humans seem to acquire HTNV infection primarily in fields. However, SEOV is carried by the brown rat, *Rattus norvegicus*, and the black rat, *R. rattus*, which are peridomestic rodents. Thus, humans tend to become infected with SEOV in cities and close to dwellings.[8,11–14] Recently, Amur virus (AMRV; also known as Soochong virus) was identified in the Korean field mouse *A. peninsulae* and in HFRS cases in China, Korea, and Far East Russia.[11–13,15,16] Thus, AMRV should also be considered as one of the causative agents of HFRS in East Asia and Far East Russia.

Morbidity of HFRS is 1.9 per 100,000 population, and about 100–200 HFRS cases are reported annually in Far East Russia.[17] In addition, seroprevalence in healthy residents in Khabarovsk and Primorsky regions is about 2.4% and 2.7%, respectively.[18,19] Despite the basic epidemiological information, an etiological analysis of HFRS has not been carried out in this region because of the close antigenicities between the viruses. Usual serological methods, such as indirect immunofluorescent antibody assays, cannot differentiate the infections caused by AMRV and HTNV. Additionally, genetic or antigenic information about the viruses circulating in the region remains extremely limited.

In the present study, we successfully isolated HTNV and AMRV from *A. agrarius* and *A. peninsulae*, respectively, in Far East Russia. Furthermore, the genetic and antigenic properties of these isolates were compared with the properties of other hantaviruses. Additionally, a serological differential diagnosis of HFRS patients in the Primorsky and Khabarovsk regions of Far East Russia was performed using a neutralization test to distinguish HTNV, AMRV, and SEOV infections.

MATERIALS AND METHODS

Rodent survey. Epizootiological surveys targeting rodents were conducted in Khekhtsir, about 20 km south from Khabarovsk, and Galkino, about 20 km east from Khabarovsk, Russia, in 2002 and 2005, respectively. Animals were captured using live traps set in forests and fields at these survey locations. Live animals were killed by cardiac puncture under anesthesia by ether inhalation, and serum was separated from the collected blood. From dead animals, blood samples were collected using filter paper. The paper was air-dried and immersed in a 10× volume of phosphate-buffered saline (PBS) at 4°C overnight, and the supernatant was used as 10× diluted serum. The sera were heat-inactivated at 56°C for 30 minutes and then stored at −40°C until use. The lungs were collected from all rodents and stored at −80°C until use.

*Address correspondence to Hiroaki Kariwa, Graduate School of Veterinary Medicine, Hokkaido University, Kita-Ku, Kita-18, Nishi-9, Sapporo, Hokkaido, Japan, 060-0818. E-mail: kariwa@vetmed.hokudai.ac.jp

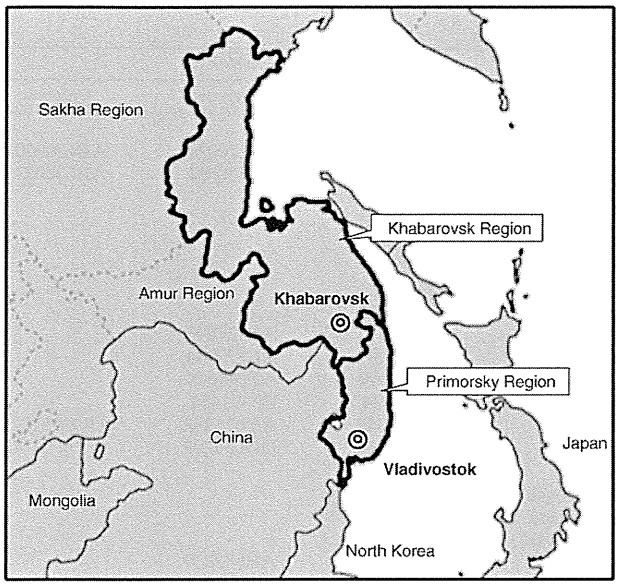

FIGURE 1. Geographical locations of epizootiological survey sites in Far East Russia. Rodents were captured in the Khabarovsk region. Sera of HFRS patients were collected in the Primorsky and Khabarovsk regions.

Human sera. Sera from 67 HFRS patients in the Khabarovsk and Primorsky regions, Russia, from 1965 to 2002 (Figure 1) were tested for neutralizing antibodies to hantaviruses. These sera were heat-inactivated and stored at −40°C until use.

Patient sera were collected with the informed consent of the patients. All experiments using patient sera were approved by the Ethics Committee of Hokkaido University and were performed in a BSL-3 laboratory at the Graduate School of Veterinary Medicine, Hokkaido University.

Cells and media. Vero E6 cells (No. CRL-1586; ATCC, Manassas, VA) were maintained in minimum essential medium with Eagle's salts (MEM; Invitrogen, Carlsbad, CA) supplemented with 10% fetal bovine serum (FBS), 2 mM L-glutamine, 100 IU/mL penicillin G, and 100 μg/mL streptomycin.

Indirect immunofluorescent antibody assay. For the detection of antihantavirus antibodies in wild rodents, immunofluorescent antibody assay (IFA) was carried out as described previously.[8] Vero E6 cells were infected separately with HTNV 76-118,[20] Bao14,[21] AMRV H5,[22] SEOV SR-11,[23] or PUUV Sotkamo, and the infected cells were fixed using cold acetone on 24-well slides. Wild rodent sera, including sera from dead animals, diluted 1:16 with PBS were spotted onto the slides and incubated at 37°C for 1 hour. The slides were washed three times with PBS, and then, Alexa Fluor 488 goat anti-mouse immunoglobulin G (IgG; Invitrogen) was applied on the slides. After 1 hour of incubation and washing, the cells were observed under a fluorescence microscope. Scattered and fine granular fluorescence in the cytoplasm of Vero E6 cells was considered to indicate a positive reaction. Positive samples were further tested to determine IFA titer, which was the reciprocal of the highest serum dilution giving the positive reaction.

For the detection of hantaviral antigens in Vero E6 cells, the inoculated cells on 24-well slides were visualized using a monoclonal antibody E5/G6 to hantavirus N[24] and Alexa Fluor 488 goat anti-mouse IgG.

Reverse transcription polymerase chain reaction. Total RNA from lung tissue of rodents or Vero E6 cells was extracted using ISOGEN (Nippon Gene Co.). Purified total RNA (5 μg) was reverse-transcribed using Superscript II RNase H reverse transcriptase (Invitrogen) and random primers (Invitrogen) according to the manufacturer's protocol. All segments of hantaviruses were amplified by polymerase chain reaction (PCR) using Platinum Taq DNA polymerase Hi Fidelity (Invitrogen). The thermal conditions for PCR were 94°C for 2 minutes followed by 35 cycles of 94°C for 30 seconds, 50–60°C (depending on the primer used) for 30 seconds, and 68°C for 2 minutes. To detect hantavirus RNA from wild rodents, primers AMR595SFw (5′-agcatgaaggcagaagagat-3′) and Bao14_840SRv (5′-ctgccgtaggtagtccctgt-3′) were used to detect HTNV, and primers AMR595SFw and AMR1252SRv (5′-ctctgtgctagtgttctcaa-3′) were used to detect AMRV.

Virus isolation. The method of hantavirus isolation has been described previously.[25] Lung tissue from both hantavirus antibody- and RNA-positive wild rodents was selected for inoculation in Vero E6 cells. Lungs of *A. agrarius* and *A. peninsulae* were homogenized in MEM using a cold pestle, mortar, and sea sand. Part (10%) of the homogenate was centrifuged (2,000 × *g* for 5 minutes), and each supernatant was inoculated in Vero E6 cells grown in a 25-cm^2 flask by centrifugation (670 × *g*) for 1 hour at room temperature. After the inoculum was discarded, the cells were cultured at 37°C in a 5% CO_2 incubator and then subcultured after a 14-day interval. At subculture, some cells were collected and spotted on 24-well slides at 37°C for 4 hours in 5% CO_2. The slides were fixed with cold acetone and used as antigen slides for IFA. The remaining collected cells were examined for hantaviral RNA by reverse transcription (RT)-PCR as described above.

Sequencing hantavirus genes. The open reading frames (ORFs) of all segments of newly isolated hantaviruses were amplified using specific primers. PCR products were extracted and purified from agarose gels using the Wizard SV Gel and PCR Clean-Up System (Promega, Fitchburg, WI) and sequenced directly using the BigDye Terminator (version 3.1) Cycle Sequencing Kit and an ABI 3130 Genetic Analyzer (Applied Biosystems, Foster City, CA) according to the manufacturer's protocol.

Genetic analysis. Hantavirus nucleotide and amino acid sequences were compared using Genetyx-mac (version 10.0; Genetyx Corp., Tokyo, Japan) for calculating nucleotide and amino acid identities among hantaviruses. MEGA 4 (available at http://www.megasoftware.net/mega.html) was used to generate multiple alignments. A GTR++I model was selected as the best probability model of Bayesian phylogenetic tree of each hantavirus genome segment by MrModeltest software (version 2.3).[26] Phylogenetic trees were drawn using MrBayes (version 3.1.2).[27] Two independent, parallel Markov chain Monte Carlo Metropolis coupling (MCMCMC) analyses, each with four chains (three heated and one cold), were computed for 0.7–1.5 million generations, with tree sampling every 100 generations. A burn-in period of 175,000–375,000 generations was discarded for each run before calculating consensus trees. After two runs of calculation, 10,500–22,500 trees were made, and these trees were used for generating the consensus tree. The sequences of hantaviruses determined in this study were downloaded from the National Center for Biotechnology Information website (http://www.ncbi.nlm.nih.gov/) and are listed in Table 1.

TABLE 1
Hantavirus sequences used in this study

Strain	Source	Capture site		Genbank ID		
		Country	Region	S segment	M segment	L segment
Newly isolated virus						
Khekhtsir/AP209/2005	*A. peninsulae*	Russia	Khabarovsk	AB620028	AB620029	AB620030
Galkino/AA57/2002	*A. agrarius*	Russia	Khabarovsk	AB620031	AB620032	AB620033
Amur virus						
Solovey/AP61/1999	*A. peninsulae*	Russia	Primorsky	AB071183	–*	–
Solovey/AP63/1999	*A. peninsulae*	Russia	Primorsky	AB071184	–	–
AP1371	*A. peninsulae*	Russia	Khabarovsk	AF427324	–	–
AP1168	*A. peninsulae*	Russia	Khabarovsk	AF427323	–	–
AP708	*A. peninsulae*	Russia	Khabarovsk	AF427322	–	–
H5	Human	China	Heilongjiang	AB127996	AB127993	
B78	Human	China	Shandong	AB127997	AB127994	–
Liu	Human	China	Shandong	AF288649	AF288648	–
JilinAP06	*A. peninsulae*	China	Jilin	EF121324	EF371454	–
SC-1	*A. peninsulae*	Korea	Gangwon	AY675349	AY675353	DQ056292
SC-2	*A. peninsulae*	Korea	Gangwon	AY675350	DQ056293	AY675354
Hantaan virus						
AA1028	*A. agrarius*	Russia	Khabarovsk	AF427318	–	–
AA1719	*A. agrarius*	Russia	Khabarovsk	AF427319	–	–
AA2499	*A. agrarius*	Russia	Khabarovsk	AF427320	–	–
KHB/HFRS/Pat#A2	Human	Russia	Khabarovsk	–	AB086620	–
KHB/HFRS/Pat#A3	Human	Russia	Khabarovsk	–	AB086619	–
KHB/HFRS/Pat#A12	Human	Russia	Khabarovsk	–	AB086621	–
Bao14	*A. agrarius*	China	Heilongjiang	AB127998	AB127995	–
CGHu1	Human	China	Guizhou	EU092218	EU092222	–
S85-46	*A. agrarius*	China	Sichuan	AF288659	AF288658	–
76-118	*A. agrarius*	Korea	Gyong Gi	NC_005218	NC_005219	NC_005222
CUMC-B11	Not known	Korea		U37768	U38117	–
CFC94-2	Human	Korea		X95007	–	–
Maaji-2	Human	Korea		AF321095	–	–
Q32	*A. agrarius*	China	Guizhou	AB027097	DQ371905	DQ371906
CGAa4MP9	*A. agrarius*	China	Guizhou	EF990915	EF990929	–
84FLi	*A. agrarius*	China	Shaanxi	AY017064	AF345636	AF336826
A9	*A. agrarius*	China	Jiangsu	AF329390	AF035831	AF293665
Z10	Human	China	Zhejiang	NC_006433	NC_006437	NC_006435
Seoul virus						
SR-11	*Rattus norvegicus*	Japan	Hokkaido	M34881	M34882	–
80-39	*R. norvegicus*	Korea	Seoul	NC_005236	NC_005237	NC_005238
Puumala virus						
Sotkamo	*Myodes glareolus*	Finland		NC_005224	NC_005223	NC_005225

* Not registered or not used in this study.

Immune sera. Antisera to each hantavirus were obtained from hantavirus-immunized mice. Two-week-old BALB/c mice (SLC, Hamamatsu, Japan) were inoculated subcutaneously (s.c.) with 3,000 focus-forming units (FFUs) of two strains of newly isolated hantaviruses. At 70 days post-inoculation (d.p.i.), mice were killed by cardiac puncture under anesthesia with sevoflurane, and the sera were collected. The sera were heat-inactivated and stored at −40°C until use.

All animal experiments were performed according to the Guidelines of Animal Experimentation of the School of Veterinary Medicine, Hokkaido University. All animal experiments were carried out in a biosafety level 3 animal facility.

Focus reduction neutralization test. The protocol for focus reduction neutralization test (FRNT) has been described previously.[28] Immune mouse sera were used to analyze serological relationships among newly isolated hantaviruses and other hantaviruses. Additionally, 67 human sera from HFRS patients in the Primorsky and Khabarovsk regions were used to identify the serotype of hantaviruses infection in each patient. Serially diluted samples (100 μL) were mixed with an equal volume of stock viruses (200 FFUs/100 μL), and these mixtures were incubated at 37°C for 1 hour in 5% CO_2. The mixtures (50 μL/well) were inoculated onto Vero E6 cell monolayers grown in 96-well plates (Nalge Nunc, Roskilde, Denmark). After adsorption for 1 hour at 37°C, the inoculum was removed, and 150 μL MEM with 1.5% carboxymethyl cellulose (CMC-MEM) were layered onto the cells and incubated at 37°C for 4 days in 5% CO_2. After incubation, the monolayers were washed with PBS, fixed with methanol, and air-dried. Foci of hantaviruses were immunostained with E5/G6 mAb and Alexa Fluor 488 goat anti-mouse IgG. Stained foci were counted under a fluorescence microscope. The neutralization titer was expressed as a reciprocal of the highest dilution that showed ≥ 80% inhibition of virus focus formation.

Statistical analysis. Statistical analysis for the comparison of the proportions of serotypes among HFRS patients living at different sites was performed using the χ^2 test. Haberman's residual analysis was conducted to examine which hantavirus was the major cause of HFRS in the Khabarovsk and Primorsky regions.[29]

RESULTS

Rodent survey. We captured 29 *A. peninsulae* in the forest of Khekhtsir close to Khabarovsk city in 2005 and

TABLE 2
Detection of antihantavirus antibodies and virus RNA in *A. peninsulae* ($N = 29$) and *A. agrarius* ($N = 47$)

Number	IFA antibody titer*				RT-PCR	Virus isolation
	AMRV H5	HTNV 76-118	SEOV SR-11	PUUV Sotkamo		
A. peninsulae						
167	256	512	< 16	< 16	+	N.D.†
172‡	**256**	**256**	**< 16**	**< 16**	**+**	**–**
186	256	512	< 16	< 16	+	N.D.
199	512	128	< 16	< 16	+	N.D.
209	**1,024**	**1,024**	**128**	**< 16**	**+**	**+**
161	512	512	< 16	< 16	–	N.D.
170	512	128	256	< 16	–	N.D.
189	1,024	128	128	< 16	–	N.D.
190	32	16	< 16	< 16	–	N.D.
191	1,024	512	512	< 16	–	N.D.
166	< 16	< 16	< 16	< 16	+	N.D.
Others ($N = 18$)	< 16	< 16	< 16	< 16	–	N.D.
A. agrarius						
56	**> 2,048**	**> 2,048**	**128**	**< 16**	**+**	**+**
57	**> 2,048**	**> 2,048**	**512**	**< 16**	**+**	**+**
61	**1,024**	**1,024**	**256**	**< 16**	**+**	**+**
65	**> 2,048**	**> 2,048**	**> 2,048**	**< 16**	**+**	**+**
54	> 2,048	> 2,048	256	< 16	–	N.D.
Others ($N = 42$)	< 16	< 16	< 16	< 16	–	N.D.

* IFA antibody titer was expressed as a reciprocal of the highest dilution that showed specific fluorescence.
† N.D. = not done.
‡ Rodent samples in bold were used for virus isolation.

47 *A. agrarius* in the field of Galkino near Khabarovsk city in 2002 (Table 2). Ten *A. peninsulae* (34.5%) and five *A. agrarius* (10.6%) were seropositive for hantaviruses. Antibody titers against AMRV in *A. peninsulae* ranged from 1:32 to 1:1,024, which was fairly comparable with the titers against HTNV. Antibody titers against SEOV were apparently lower than the titers against AMRV in 8 of 10 seropositive *A. peninsulae*. Antibody titers against HTNV in the five seropositive *A. agrarius* ranged from 1:1,024 to more than 1:2,048, which was equivalent to the titers against AMRV. Four of five seropositive *A. agrarius* had IFA antibody titers against AMRV or HTNV that were more than or equal to fourfold greater than the titers against SEOV. No antibody was detected against Puumala virus (PUUV) in any animal. Lung samples of all 76 rodents were tested for the hantavirus S gene by RT-PCR (Table 2). Six *A. peninsulae* (20.7%) and four *A. agrarius* (8.5%) contained virus RNA.

Virus isolation. Virus isolation was carried out using two lung samples of *A. peninsulae* (numbers 172 and 209) and four samples of *A. agrarius* (numbers 56, 57, 61, and 65) that were sero- and RNA-positive. Lung homogenates of each sample were inoculated on Vero E6 cells. At 14 d.p.i., hantavirus RNA was detected from cells inoculated with *A. peninsulae* number 209 and *A. agrarius* numbers 56, 57, 61, and 65. Hantavirus N was detected at 42 d.p.i. (*A. peninsulae* number 209) and 28 d.p.i. (*A. agrarius* numbers 56, 57, 61, and 65). Thus, five strains of hantavirus were isolated from wild rodents (Table 2). Hantavirus isolates from *A. peninsulae* number 209 and *A. agrarius* numbers 56, 57, 61, and 65 were designated Khekhtsir/AP209/2005 (AP209), Galkino/AA56/2002 (AA56), Galkino/AA57/2002 (AA57), Galkino/AA61/2002 (AA61), and Galkino/AA65/2002 (AA65), respectively. AP209 and AA57 were used for additional genetic and antigenic characterization.

Genetic analysis of hantavirus isolates. Nucleotide sequences covering the ORF of all segments from AP209 and AA57 were determined. The sequences determined and used in this study are listed in Table 1.

The S segment of AP209 was quite similar to the segments of AMRV Solovey/AP61/1999 and Solovey/AP63/1999 that were detected from *A. peninsulae* in the Primorsky region, Russia (96.0–96.3% nucleotide identity and 99.3–99.8% amino acid identity) (Table 3). The identities in the S segment between AP209 and AMRVs from North East China and Korea (H5, B78, and SC-1) were slightly lower (90.1–90.5% nucleotide identity and 98.8–99.5% amino acid identity) (Table 3). The nucleotide identities of the S segment between AMRV and other hantaviruses such as HTNV, SEOV, and PUUV were much lower at 82.6–85.8%, 73.8–74.8%, and 63.9–64.3%, respectively. The M and L segments of AP209 were closest to the identities of AMRVs (M segment, 87.5–93.6% and 96.7–98.9%; L segment, 88.9–89.4% and 98.7–99.0% for nucleotide and amino acid identities, respectively) (Table 3) among hantaviruses. Thus, isolate AP209 was identified as AMRV.

The nucleotide and amino acid sequences of all genome segments of AA57 were quite similar to the sequences of HTNV strain Bao14, which was isolated from an HFRS patient in Heilongjiang, China (S segment, 98.4% and 99.8%; M segment, 97.0% and 99.0%; L segment, 97.3% and 99.7% nucleotide and amino acid identities, respectively) (Table 3). Thus, isolate AA57 was identified as HTNV. Additionally, a comparison of the M segments between AA57 and hantavirus sequences from HFRS patients in the Khabarovsk region (KHB/HFRS/PAT#A2, KHB/HFRS/PAT#A3, and KHB/HFRS/PAT#A12)[12] showed 96–99% identity at the nucleotide level. The nucleotide identities of the S, M, and L segments between AA57 and other HTNVs (76-118, A9, and Z10) ranged from 85.5% to 88.8%, from 84.0% to 87.6%, and from 83.3% to 88.0%, respectively (Table 3).

Phylogenetic analyses of hantavirus S, M, and L segments were performed (Figure 2). Previously, the work by Zou and others[30] described that the Hantaan superclade, including HTNV and AMRV, was divided into several lineages, and the S, M, and L segments of AMRV occupied lineages S6, M6, and L5, respectively. In the present study, the S, M, and

TABLE 3

Nucleotide (ORF region) and amino acid identities* among the two hantavirus isolates (Khekhtsir AP209 and Galkino AA57) and other hantaviruses

	AMRV						HTNV					SEOV		PUUV
Strain	Khekhtsir AP209	Solovey AP61	Solovey AP63	H5	B78	SC-1	Galkino AA57	Bao14	76-118	A9	Z10	SR-11	80-39	Sotkamo
S segment														
Khekhtsir AP209	–	96.3	96.0	90.1	90.1	90.5	85.1	85.8	83.0	83.0	83.6	74.8	74.1	63.9
Solovey AP61	99.8	–	99.1	90.2	90.2	90.4	84.5	85.2	82.7	82.8	83.5	73.9	74.1	64.1
Solovey AP63	99.3	99.5	–	90.1	90.1	90.4	84.2	84.9	82.8	82.6	83.4	73.8	74.0	64.3
H5	98.8	99.1	98.6	–	100.0	91.5	83.8	83.9	83.2	82.9	83.4	74.6	73.9	64.2
B78	98.8	99.1	98.6	100.0	–	91.5	83.8	83.9	83.2	82.9	83.4	74.6	73.9	64.2
SC-1	99.5	99.8	99.3	98.8	98.8	–	83.7	84.1	83.0	84.1	84.1	74.1	73.8	64.0
Galkino AA57	97.7	97.9	97.4	97.4	97.4	97.7	–	98.4	88.8	85.5	86.4	74.3	74.7	63.5
Bao14	97.4	97.7	97.2	97.7	97.7	97.4	99.8	–	89.0	86.2	86.7	74.5	74.7	63.2
76-118	96.5	96.7	96.3	96.7	96.7	96.5	98.8	99.1	–	84.8	85.8	74.3	74.6	63.0
A9	96.0	96.3	95.8	96.3	96.3	96.0	97.4	97.7	96.7	–	89.5	75.0	74.5	64.2
Z10	97.0	97.2	96.7	97.2	97.2	97.0	97.9	98.1	97.2	97.2	–	75.0	75.1	62.5
SR-11	82.1	82.1	81.6	81.6	81.6	81.8	82.3	82.1	82.3	80.9	81.1	–	97.6	62.0
80-39	83.0	83.0	82.5	82.5	82.5	82.8	83.2	83.0	83.2	81.8	82.1	98.4	–	62.0
Sotkamo	60.5	60.5	60.3	60.7	60.7	60.3	60.5	60.7	60.7	59.8	60.0	61.7	61.9	–
M segment														
Khekhtsir AP209	–	–	–	93.6	93.1	87.5	81.2	81.2	81.1	80.3	80.1	72.3	71.8	59.3
H5	98.9	–	–	–	96.5	87.0	79.9	79.9	79.8	79.4	79.8	71.7	71.2	60.1
B78	98.7	–	–	99.1	–	87.0	80.4	80.4	79.6	79.7	79.5	71.6	71.3	59.9
SC-1	96.7	–	–	96.9	97.1	–	80.6	80.3	80.5	79.4	80.0	72.2	71.7	59.4
Galkino AA57	92.4	–	–	92.7	92.3	91.7	–	97.0	87.6	84.0	85.0	72.0	71.8	60.1
Bao14	92.3	–	–	92.5	92.2	91.5	99.0	–	87.7	84.4	85.1	72.3	71.9	59.8
76-118	92.3	–	–	92.2	92.0	91.1	97.5	97.9	–	84.6	84.3	72.5	72.0	60.1
A9	91.6	–	–	91.5	91.2	90.6	94.7	95.0	95.4	–	87.3	71.8	71.6	60.4
Z10	92.0	–	–	91.9	91.5	90.7	94.9	95.0	95.3	96.2	–	71.6	71.6	60.0
SR-11	76.5	–	–	76.8	76.3	76.4	76.6	76.8	77.0	76.3	76.4	–	96.5	60.8
80-39	76.8	–	–	77.0	76.4	76.6	76.8	77.0	77.1	76.3	76.4	98.9	–	60.7
Sotkamo	54.3	–	–	54.5	54.4	53.9	53.8	53.6	53.8	53.6	53.7	53.8	53.8	–
L segment		–	–											
Khekhtsir AP209	–	–	–	89.4	–	88.9	81.9	81.9	81.5	81.6	82.2	–	75.6	67.5
H5	99.0	–	–	–	–	88.6	81.6	81.2	81.7	81.0	81.8	–	75.4	67.7
SC-1	98.7	–	–	98.7	–	–	95.9	81.1	81.3	81.1	81.4	–	75.3	67.4
Galkino AA57	96.1	–	–	96.0	–	81.2	–	97.3	88.0	83.4	84.0	–	74.9	67.3
Ba014	96.1	–	–	95.9	–	95.8	99.7	–	88.1	83.2	84.0	–	74.8	67.2
76-118	95.7	–	–	95.8	–	95.6	98.7	98.6	–	83.6	83.5	–	74.3	66.8
A9	94.2	–	–	94.3	–	93.9	95.8	95.6	95.6	–	85.4	–	74.7	67.1
Z10	95.5	–	–	95.5	–	95.3	97.6	97.5	97.3	96.1	–	–	74.9	67.3
80-39	85.5	–	–	85.3	–	85.3	85.4	85.4	85.0	83.7	85.4	–	–	67.7
Sotkamo	69.1	–	–	68.7	–	68.7	69.1	69.0	68.9	67.9	69.3	–	68.5	–

*Values to the right above the diagonal show nucleotide identities; values to the left below the diagonal show amino acid identities.

L segments of AP209 clustered with AMRVs in lineages S6, M6, and L5, respectively, consistent with the results in the work by Zou and others.[30] AP209 was more related to AMRVs detected in the Primorsky region of Far East Russia, such as AP708, AP1371, AP1168, Solovey/AP61/1999, and Solovey/AP63/1999, than AMRVs from China and Korea. Although the M and L segments of AMRV clustered in distinct lineages from other HTNVs, the S segment of AMRV clustered within HTNV. The S, M, and L segments of strain AA57 clustered with HTNVs from the Primorsky region (AA1028, AA1719, and AA2499) and HTNVs from China (Bao14 and CGHu1), which consist of the Far East (FE) genotype within HTNVs.[13,28] Interestingly, strain CGHu1 isolated from Guizhou, a southern province of China, also clustered with the FE genotype. HTNV lineages in S1 were divided into S1-a and S1-b sublineages according to their geographical origins: S1-a from Korea (76-118, CUMC-B11, and Maaji-2) and S1-b from Far East Russia (AA57, AA1028, AA1719, and AA2499) and China (Bao14 and CGHu1). The same clustering patterns were also observed with the M and L segments.

Antigenic characterization. The antigenic characterization of AP209, AA57, and other hantaviruses was performed using a neutralization test (Table 4). Anti-AMRV mouse sera had more than fourfold higher titers against AMRV strains H5 and AP209 than those titers against HTNV and SEOV. Anti-AA57 mouse serum had a more than fourfold higher neutralization titer against AA57 compared with those titers against AMRVs and SEOV. These results indicate that the antigenicities of AMRV, HTNV, and SEOV are different and that the neutralization test may be useful in the differential diagnosis of HFRS caused by AMRV, HTNV, or SEOV in Far East Russia.

Serological analysis of patient sera. To examine the causative agents of HFRS in the Khabarovsk and Primorsky regions, the neutralization test was performed on a total of 67 HFRS patients who had IFA antibodies to hantaviruses (Tables 5 and 6). The hantavirus in each HFRS patient was determined as a certain virus giving a neutralization titer more than or equal to fourfold higher than the titer of other viruses (Tables 5 and 6). If the neutralization titer difference was less than fourfold, we considered the infected hantavirus of the sample to be untyped. If the neutralization titer was less than 1:20 for any hantaviruses, we regarded the sample as negative for hantavirus infection. Of 67 HFRS patients, 14, 13, and 15 were

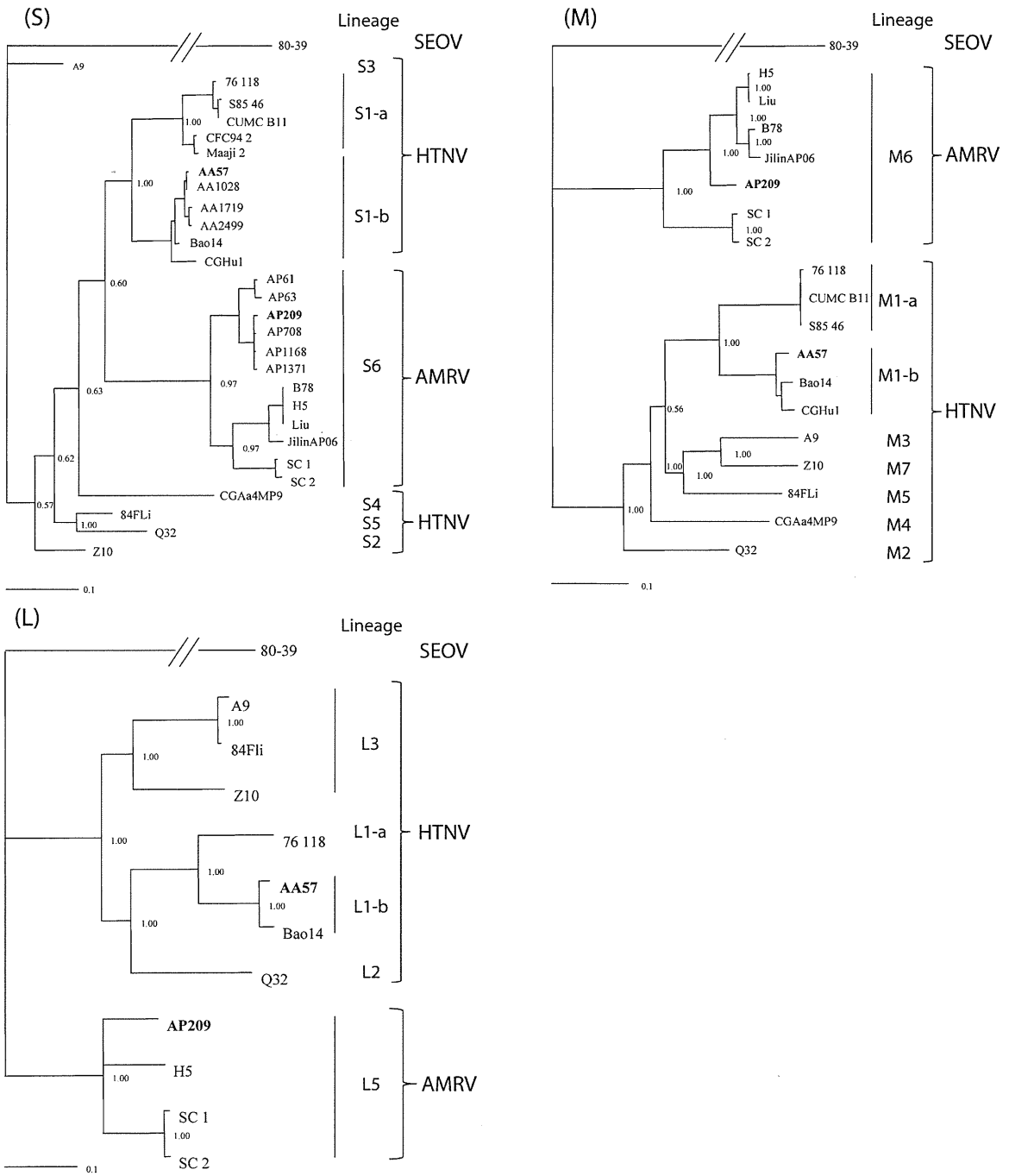

FIGURE 2. Phylogenetic consensus trees of hantaviruses based on nucleotide sequences covering the entire ORF of the S, M, and L segments. The trees were generated using MCMCMC analyses. The reliability of the tree was evaluated by the posterior probability value derived from MrBayes. The scale bar indicates 0.1 nucleotide substitutions per site.

diagnosed as AMRV (20.9%), HTNV (19.4%), and SEOV (22.4%) infections, respectively, and 25 patients (37.3%) were untyped (Tables 5 and 6). All of 20 untyped sera in Khabarovsk region showed strong cross-reaction to AMRV and HTNV (Table 6). The seroprevalence of AMRV, HTNV, and SEOV in HFRS patients differed with each sampling site (χ^2 value = 70.69, degrees of freedom [df] = 6, $P < 0.001$). SEOV (60.0%; $P < 0.001$) and AMRV (81.8%; $P < 0.001$) were the major causative agents of HFRS in Vladivostok city and the rural areas of Primorsky region except Vladivostok, respectively (Table 5). HTNV (35.5%; $P < 0.002$) may be one of the major causes in the Khabarovsk region (Table 6).

DISCUSSION

Previous investigations of HFRS patients in Far East Russia have revealed that AMRV, HTNV, and SEOV are causative agents of HFRS in this region.[12,13] However, no complete

TABLE 4

Antigenic characterization of Khekhtsir AP209 and Galkino AA57 by cross-neutralization test using immune mouse sera

Antisera		Neutralization titer*			
		AMRV		HTNV	SEOV
Virus	Strain	H5	Khekhtsir AP209	Galkino AA57	SR-11
AMRV	H5	80	80	20	< 20
AMRV	Khekhtsir AP209	320	640	40	20
HTNV	Galkino AA57	640	640	2,560	40
SEOV	SR-11	< 20	< 20	< 20	40

* Neutralization titer was expressed as a reciprocal of the highest dilution that showed 80% or more inhibition of virus focus formation.

etiological analysis of each HFRS patient to identify the infected hantavirus has been conducted. Because the biological properties of hantaviruses in this region have not been well-characterized, a differential diagnosis of infected viruses in HFRS is quite difficult. Thus, we isolated hantaviruses in Far East Russia and characterized the new isolates. Additionally, serological differential diagnoses were carried out on HFRS patients in this region to identify the virus in each infected patient.

TABLE 5

Differential diagnosis of HFRS patients in the Primorsky region by neutralization test

Patient number	Days after onset	Neutralization titer: AMRV Khekhtsir AP209	HTN Galkino AA57	SEOV SR-11	Infected virus
Vladivostok city					
1	14	< 20*	< 20	40	SEOV
2	11	< 20	< 20	40	SEOV
3	11	20	20	80	SEOV
4	17	20	< 20	160	SEOV
5	16	40	< 20	40	UT†
6	8	< 20	< 20	40	SEOV
7	9	40	20	160	SEOV
8	12	40	40	320	SEOV
9	25	640	80	20	AMRV
10	26	20	20	160	SEOV
11	14	< 20	40	< 20	HTNV
12	20	20	20	80	SEOV
13	11	< 20	40	< 20	HTNV
14	28	< 20	80	80	UT
15	17	20	20	80	SEOV
16	17	1,280	80	< 20	AMRV
17	730	40	20	160	SEOV
18	60	80	20	< 20	ARMV
19	17	< 20	< 20	80	SEOV
20	8	< 20	< 20	40	SEOV
21	10	20	< 20	80	SEOV
22	28	< 20	< 20	40	SEOV
23	8	20	< 20	20	UT
24	13	320	< 20	< 20	AMRV
25	26	1,280	80	20	AMRV
Outside Vladivostok					
26	20	1,280	160	20	AMRV
28	6	320	40	20	AMRV
29	5	1,280	320	40	AMRV
30	13	160	40	< 20	AMRV
32	9	1,280	160	20	AMRV
33	32	80	160	< 40	UT
35	17	1,280	160	40	AMRV
36	15	640	80	< 20	AMRV
37	20	640	160	40	AMRV
38	16	< 40	< 40	40	UT
39	22	1,280	320	20	AMRV

* 80% focus reduction method.
† Untyped.

TABLE 6

Differential diagnosis of HFRS patients in the Khabarovsk region by neutralization test

Patient no.	Months after onset	Neutralization titer: AMRV Khekhtsir AP209	HTNV Galkino AA57	SEOV SR-11	Infected virus
1	142	40	160	20	HTNV
2	71	40	80	< 20	UT
3	48	160	160	20	UT
5	13	320	1,280	< 20	HTNV
6	5	160	320	40	UT
7	18	160	160	20	UT
8	17	160	640	40	HTNV
9	3	80	320	20	HTNV
10	4	80	160	20	UT
11	144	320	320	40	UT
12	6	160	160	< 20	UT
13	3	40	160	< 20	HTNV
14	5	80	320	20	HTNV
15	5	160	320	20	UT
16	4	40	80	< 20	UT
17	13	80	160	< 20	UT
18	3	80	160	< 20	UT
19	3	40	160	< 20	HTNV
20	4	1,280	5,120	40	HTNV
21	4	80	160	20	UT
22	4	160	160	20	UT
23	4	320	1,280	20	HTNV
24	2	320	320	< 20	UT
25	1	80	320	20	HTNV
26	2	80	80	< 20	UT
27	396	80	320	20	HTNV
28	2	160	160	< 20	UT
29	1	80	160	< 20	UT
30	2	160	320	< 20	UT
31	168	160	160	< 20	UT
32	288	160	320	20	UT

Rodent surveys were carried out in rural areas of the Khabarovsk region, and we confirmed that HTNV and AMRV were maintained in *A. agrarius* and *A. peninsulae*, respectively, which we have described previously for hantavirus infection in rodents of the Primorsky region, Russia.[8,11] These results indicated that HTNV and AMRV are distributed throughout Far East Russia.

We successfully isolated four strains of HTNV and one strain of AMRV. Among the isolates, HTNV strain AA57 from *A. agrarius* and AMRV strain AP209 were subjected to genetic and antigenic characterization. AA57 was genetically closely related to the sequences from HFRS patients in the Khabarovsk region[12] and Bao14, which was isolated from HFRS patients in China. Newly isolated AMRV AP209 from *A. peninsulae* was genetically closely related to the sequences from rodents and HFRS patients in the Primorsky region. These results indicate that HTNV and AMRV are the causative agents of HFRS in the Khabarovsk region. Although the M and L segments of AMRV and HTNV clustered in distinct lineages, the S segment of AMRV was included in HTNV. This observation was also reported in the work by Zou and others.[30] Previous reports of phylogenetic analysis have indicated that a natural reassortment occurred between HTNV and SEOV in China and among different lineages of PUUVs in nature.[31,32] Additionally, dual infection with Sin Nombre virus and Black Creek Canal virus could produce reassortant viruses under experimental conditions.[33] Other reports have described that a recombination of the virus genome occurred in Dobrava virus and Saaremaa virus and in different lineages of Tula

viruses in nature.[34,35] Thus, it is feasible that some discontinuous mutation, such as reassortment, may have occurred between AMRV and HTNV as indicated between HTNV and SEOV in China.[32]

In the cross-neutralization test using immune sera against HTNV, AMRV, and SEOV, the immune sera had fourfold higher titers against the homologous virus than the heterologous viruses. This result indicates that the cross-neutralization test is useful for the differential diagnosis of AMRV, HTNV, and SEOV infection in Far East Russia.

To obtain more information about HFRS etiology and epidemiology in Far East Russia, the neutralization tests were carried out using HFRS patient sera from the Primorsky and Khabarovsk regions. The results showed that AMRV (20.9%), HTNV (19.4%), and SEOV (22.4%) were the causative agents of HFRS in Far East Russia, and these findings are consistent with the results of previous reports.[13] However, the major cause of HFRS varied according to location. SEOV was the most common cause of HFRS in Vladivostok city in the Primorsky region (15/25). In Vladivostok city, *R. norvegicus* and *R. rattus* may transmit SEOV to city residents (Table 5). Some patients in Vladivostok were infected with AMRV and HTNV (5/25 and 2/25, respectively). Russian people frequently visit vegetable gardens in rural areas called dachas to cultivate plants. Because *A. peninsulae* and *A. agrarius* may live in forests and fields near dachas, it is highly possible that people, including city residents, may acquire AMRV or HTNV infection close to dachas. Interestingly, in the rural area of the Primorsky region, most patients were infected with AMRV (9/11) (Table 5). It is possible that people in this area may become infected more frequently with AMRV in forests that *A. peninsulae* inhabit. However, in the Khabarovsk region, HTNV may be the major cause of HFRS (Table 6). AMRV infection may occur in the Khabarovsk region, although no AMRV-specific antibodies were detected in this study. There are three possible explanations for negative results of AMRV-specific antibodies. (1) Residents in Khabarovsk region may contact more frequently with *A. agrarius* than *A. peninsulae*. (2) Because of the similar antigenicity between AMRV and HTNV, AMRV-infected patients may produce antibodies cross-reacted to HTNV. Most patient sera from the Khabarovsk region were collected in late convalescent phase (Table 6), which may have influenced the results of neutralization test. (3) The possibility of dual infections with AMRV and HTNV cannot be ruled out. However, because *A. agrarius* and *A. peninsulae* preferentially inhibit grass field and forest, respectively, the possibility of the dual infection at the same time may be extremely low. In addition, consecutive infections of the two viruses may not occur, because patients infected with AMRV or HTNV can produce cross-neutralizing antibodies to the homologous and heterologous viruses. Additional studies should be conducted to develop a clear picture of HFRS epidemiology on a larger scale. Unfortunately, in some patients (25/71), we could not differentiate the infecting hantavirus. Serotype-specific conformational epitopes have been detected in the center and C-terminal regions of the N.[24,36] Thus, a serotyping system using N-terminal truncated N could be a solution for the differential diagnosis of hantavirus infections.[37,38]

In conclusion, new isolates of AMRV and HTNV were characterized, and AMRV, HTNV, and SEOV infections were differentiated in HFRS patients of Far East Russia. The major cause of HFRS varied by location in the region: SEOV for Vladivostok city in the Prymorsky region, AMRV in the rural areas of the Primorsky region, and probably HTNV for the Khabarovsk region. Additional study is necessary to determine the risk factors of HFRS for each pathogenic virus in Far East Russia.

Received May 9, 2011. Accepted for publication November 26, 2011.

Acknowledgments: The authors thank Dr. Vladimir A. Demenev for arranging the sampling of HFRS patient sera. We appreciate all of the people who worked with us in the field in the Khabarovsk region helping with rodent trapping and supporting the surveys.

Financial support: This study was supported financially by grants-in-aid for scientific research (B) from the Ministry of Education, Culture, Sports, Science, and Technology of Japan, a scientific grant for Research on Emerging and Re-emerging Infectious Diseases from the Ministry of Health, Welfare, and Labour of Japan, and a grant from the Program of Global Center of Excellence Program, Hokkaido University ("Establishment of International Collaboration Centers for Zoonosis Control").

Authors' addresses: Hiroaki Kariwa, Keisuke Yoshikawa, Yoichi Tanikawa, Takahiro Seto, Takahiro Sanada, Ngonda Saasa, Kentaro Yoshii, and Ikuo Takashima, Graduate School of Veterinary Medicine, Hokkaido University, Sapporo, Japan, E-mails: kariwa@vetmed.hokudai.ac.jp, canis-familiaris-l@k.vodafone.ne.jp, tanikawa.yf@om.asahi-kasei.co.jp, setotaka@vetmed.hokudai.ac.jp, sanada-t@vetmed.hokudai.ac.jp, nsaasa@yahoo.co.uk, kyoshii@vetmed.hokudai.ac.jp, and takasima@vetmed.hokudai.ac.jp. Leonid I. Ivanov, Plague Control Station of Khabarovsk, Khabarovsk, Russia, E-mail: chum@chum.khv.ru. Raisa Slonova, Research Institute of Epidemiology and Microbiology, Siberian Branch of Russian Academy of Medical Sciences, Vladivostok, Russia, E-mail: atavalk@inbox.ru. Tatyana A. Zakharycheva, Far Eastern State Medical University, Khabarovsk, Russia, E-mail: dolika@inbox.ru. Ichiro Nakamura, Research Center for Zoonosis Control, Hokkaido University, Sapporo, Japan, E-mail: inaka@czc.hokudai.ac.jp. Kumiko Yoshimatsu and Jiro Arikawa, Graduate School of Medicine, Hokkaido University, Sapporo, Japan, E-mails: yosimatu@med.hokudai.ac.jp and j_arika@med.hokudai.ac.jp.

REFERENCES

1. Krüger DH, Ulrich R, Lundkvist A, 2001. Hantavirus infections and their prevention. *Microbes Infect 3:* 1129–1144.
2. Schmaljohn CS, Hjelle B, 1997. Hantaviruses: a global disease problem. *Emerg Infect Dis 3:* 95–104.
3. Jonsson CB, Schmaljohn CS, 2001. Replication of hantavirus. Schmaojohn CS, Nichol ST, eds. *Hantavirus.* Berlin, Germany: Springer-Verlag, 15–32.
4. Jonsson CB, Figueiredo LTM, Vapalahti O, 2010. A global perspective on hantavirus ecology, epidemiology, and disease. *Clin Microbiol Rev 23:* 412–441.
5. Elliot RM, Beaty BJ, Calisher CH, Goldbach RW, Nichol ST, Plyusnin A, Schmaljohn CS, 2005. Family *Bunyaviridae.* Fauquet CM, Mayo MA, Maniloff J, Desselberger U, Ball LA, eds. *Virus Taxonomy.* London, United Kingdom: Elsevier Academic Press, 695–715.
6. Zhang YZ, Zou Y, Fu ZF, Plyusnin A, 2010. Hantavirus infections in humans and animals, China. *Emerg Infect Dis 16:* 1195–1203.
7. Song JY, Chun BC, Kim SD, Baek LJ, Kim SH, Sohn JW, Cheong HJ, Kim WJ, Park SC, Kim MJ, 2006. Epidemiology of hemorrhagic fever with renal syndrome in endemic area of the Republic of Korea, 1995–1998. *J Korean Med Sci 21:* 614–620.
8. Kariwa H, Lokugamage K, Lokugamage N, Miyamoto H, Yoshii K, Nakauchi M, Yoshimatsu K, Arikawa J, Ivanov LI, Iwasaki T, Takashima I, 2007. A comparative epidemiological study of hantavirus infection in Japan and far east Russia. *Jpn J Vet Res 54:* 145–161.
9. Kariwa H, Zhong CB, Araki K, Yoshimatsu K, Lokugamage K, Lokugamage N, Murphy ME, Mizutani T, Arikawa J,

Fukushima H, Xiong H, Jiehua C, Takashima I, 2001. Epizootiological survey of hantavirus among rodent species in Ningxia Hui Autonomous Province, China. *Jpn J Vet Res 49:* 105–114.
10. Song G, Hang CS, Liao HX, Fu JL, Gao GZ, Qiu HL, Zhang QF, 1984. Antigenic difference between viral strains causing classical and mild types of epidemic hemorrhagic fever with renal syndrome in China. *J Infect Dis 150:* 889–894.
11. Lokugamage K, Kariwa H, Hayasaka D, Cui BZ, Iwasaki T, Lokugamage N, Ivanov LI, Volkov VI, Demenev VA, Slonova R, Kompanets G, Kushnaryova T, Kurata T, Maeda K, Araki K, Mizutani T, Yoshimatsu K, Arikawa J, Takashima I, 2002. Genetic characterization of hantaviruses transmitted by the Korean field mouse (*Apodemus peninsulae*), far east Russia. *Emerg Infect Dis 8:* 768–776.
12. Miyamoto H, Kariwa H, Araki K, Lokugamage K, Hayasaka D, Cui BZ, Lokugamage N, Ivanov LI, Mizutani T, Iwasa MA, Yoshimatsu K, Arikawa J, Takashima I, 2003. Serological analysis of hemorrhagic fever with renal syndrome (HFRS) patients in far eastern Russia and identification of the causative hantavirus genotype. *Arch Virol 148:* 1543–1556.
13. Yashina LN, Patrushev NA, Ivanov LI, Slonova RA, Mishin VP, Kompanez GG, Zdanovskaya NI, Kuzina II, Safronov PF, Chizhikov VE, Schmaljohn C, Netesov SV, 2000. Genetic diversity of hantaviruses associated with hemorrhagic fever with renal syndrome in the far east of Russia. *Virus Res 70:* 31–44.
14. Yashina L, Mishin V, Zdanovskaya N, Schmaljohn C, Ivanov L, 2001. A newly discovered variant of a hantavirus in *Apodemus peninsulae*, far eastern Russia. *Emerg Infect Dis 7:* 912–913.
15. Lokugamage K, Kariwa H, Lokugamage N, Iwasa M, Hagiya T, Araki K, Tachi A, Mizutani T, Yoshimatsu K, Arikawa J, Iwasaki T, Takashima I, 2004. Comparison of virulence of various hantaviruses related to hemorrhagic fever with renal syndrome in newborn mouse model. *Jpn J Vet Res 51:* 143–149.
16. Baek LJ, Kariwa H, Lokugamage K, Yoshimatsu K, Arikawa J, Takashima I, Kang JI, Moon SS, Chung SY, Kim EJ, Kang HJ, Song KJ, Klein TA, Yanagihara R, Song JW, 2006. Soochong virus: an antigenically and genetically distinct hantavirus isolated from *Apodemus peninsulae* in Korea. *J Med Virol 78:* 290–297.
17. Garanina SB, Platonov AE, Zhuravlev VI, Murashkina AN, Yakimenko VV, Korneev AG, Shipulin GA, 2009. Genetic diversity and geographic distribution of hantaviruses in Russia. *Zoonoses Public Health 56:* 297–309.
18. Ivanov LI, Liberova RN, Zdanovskaya NI, Denisov EA, Prosina NA, 1996. Contingents of people for specific prevention of hemorrhagic fever with renal syndrome in the Khabarovsk Territory and Jewish Autonomous Region of Russia. *Far East Med J 4 (Suppl Vaccination):* 44–48.
19. Kompanets GG, Slonova RA, Kushnareva TV, Maksema IG, Pysina TV, Kraeva LS, 2006. Humoral immune response to hantaviruses in health people of the Maritime Territory of Russia. *Zh Microbiol (Moscow) 3 (Suppl):* 84–87.
20. Lee HW, Lee PW, Johnson KM, 1978. Isolation of the etiologic agent of Korean Hemorrhagic fever. *J Infect Dis 137:* 298–308.
21. Wang H, Yoshimatsu K, Ebihara H, Ogino M, Araki K, Kariwa H, Wang Z, Luo Z, Li D, Hang C, Arikawa J, 2000. Genetic diversity of hantaviruses isolated in china and characterization of novel hantaviruses isolated from *Niviventer confucianus* and *Rattus rattus*. *Virology 278:* 332–345.
22. Liang M, Li D, Xiao SY, Hang C, Rossi CA, Schmaljohn CS, 1994. Antigenic and molecular characterization of hantavirus isolates from China. *Virus Res 31:* 219–233.
23. Kitamura T, Morita C, Komatsu T, Sugiyama K, Arikawa J, Shiga S, Takeda H, Akao Y, Imaizumi K, Oya A, Hashimoto N, Urasawa S, 1983. Isolation of virus causing hemorrhagic fever with renal syndrome (HFRS) through a cell culture system. *Jpn J Med Sci Biol 36:* 17–25.
24. Yoshimatsu K, Arikawa J, Tamura M, Yoshida R, Lundkvist A, Niklasson B, Kariwa H, Azuma I, 1996. Characterization of the nucleocapsid protein of Hantaan virus strain 76-118 using monoclonal antibodies. *J Gen Virol 77:* 695–704.
25. Kariwa H, Arikawa J, Takashima I, Isegawa Y, Yamanishi K, Hashimoto N, 1994. Enhancement of infectivity of hantavirus in cell culture by centrifugation. *J Virol Methods 49:* 235–244.
26. Nylander JAA, 2004. *MrModeltest v2.* Available at: http://www.abc.se/~nylander/mrmodeltest2/mrmodeltest2.html. Accessed May 22, 2008.
27. Huelsenbeck JP, Ronquist F, 2001. MRBAYES: Bayesian inference of phylogenetic trees. *Bioinformatics 17:* 754–755.
28. Lokugamage K, Kariwa H, Lokugamage N, Miyamoto H, Iwasa M, Hagiya T, Araki K, Tachi A, Mizutani T, Yoshimatsu K, Arikawa J, Takashima I, 2004. Genetic and antigenic characterization of the Amur virus associated with hemorrhagic fever with renal syndrome. *Virus Res 101:* 127–134.
29. Shelby JH, 1973. The analysis of residuals in cross classified tables. *Biometrics 29:* 205–220.
30. Zou Y, Hu J, Wang ZX, Wang DM, Li MH, Ren GD, Duan ZX, Fu ZF, Plyusnin A, Zhang YZ, 2008. Molecular diversity and phylogeny of Hantaan virus in Guizhou, China: evidence for Guizhou as a radiation center of the present Hantaan virus. *J Gen Virol 89:* 1987–1997.
31. Razzauti M, Plyusnina A, Henttonen H, Plyusnin A, 2008. Accumulation of point mutations and reassortment of genomic RNA segments are involved in the microevolution of Puumala hantavirus in a bank vole (*Myodes glareolus*) population. *J Gen Virol 89:* 1649–1660.
32. Zou Y, Hu J, Wang ZX, Wang DM, Yu C, Zhou JZ, Fu ZF, Zhang YZ, 2008. Genetic characterization of hantaviruses isolated from Guizhou, China: evidence for spillover and reassortment in nature. *J Med Virol 80:* 1033–1041.
33. Rodriguez LL, Owens JH, Peters CJ, Nichol ST, 1998. Genetic reassortment among viruses causing hantavirus pulmonary syndrome. *Virology 242:* 99–106.
34. Klempa B, Schmidt HA, Ulrich R, Kaluz S, Labuda M, Meisel H, Hjelle B, Krüger DH, 2003. Genetic interaction between distinct Dobrava hantavirus subtypes in *Apodemus agrarius* and *A. flavicollis* in nature. *J Virol 77:* 804–809.
35. Sibold C, Meisel H, Krüger DH, Labuda M, Lysy J, Kozuch O, Pejcoch M, Vaheri A, Plyusnin A, 1999. Recombination in Tula hantavirus evolution: analysis of genetic lineages from Slovakia. *J Virol 73:* 667–675.
36. Ruo SL, Sanchez A, Elliott LH, Brammer LS, McCormick JB, Fisher-Hoch SP, 1991. Monoclonal antibodies to three strains of hantaviruses: Hantaan, R22, and Puumala. *Arch Virol 119:* 1–11.
37. Araki K, Yoshimatsu K, Ogino M, Ebihara H, Lundkvist A, Kariwa H, Takashima I, Arikawa J, 2001. Truncated hantavirus nucleocapsid proteins for serotyping Hantaan, Seoul, and Dobrava hantavirus infections. *J Clin Microbiol 39:* 2397–2404.
38. Nakamura I, Yoshimatsu K, Lee BH, Okumura M, Taruishi M, Araki K, Kariwa H, Takashima I, Arikawa J, 2008. Development of a serotyping ELISA system for Thailand virus infection. *Arch Virol 153:* 1537–1542.

Virus Research 163 (2012) 486–494

Contents lists available at SciVerse ScienceDirect

Virus Research

journal homepage: www.elsevier.com/locate/virusres

Genetic diversity of hantaviruses in Mexico: Identification of three novel hantaviruses from Neotominae rodents

Hiroaki Kariwa[a,*], Haruka Yoshida[a], Cornelio Sánchez-Hernández[b], María de Lourdes Romero-Almaraz[b], José Alberto Almazán-Catalán[b], Celso Ramos[c], Daisuke Miyashita[a], Takahiro Seto[a], Ayako Takano[a], Masashi Totani[a], Ryo Murata[a], Ngonda Saasa[a], Mariko Ishizuka[a], Takahiro Sanada[a], Kentaro Yoshii[a], Kumiko Yoshimatsu[d], Jiro Arikawa[a], Ikuo Takashima[a]

[a] *Graduate School of Veterinary Medicine, Hokkaido University, Kita-18, Nishi-9, Kita-Ku, Sapporo 060-0818, Hokkaido, Japan*
[b] *Instituto de Biología, Universidad Nacional Autónoma de México, Apdo. Postal 70-153, 04510 México, D.F., Mexico*
[c] *Instituto Nacional de Salud Pública, Ave. Universidad 655, Colonia Santa Ahuacatitlán, 62508 Cuernavaca, Morelos, Mexico*
[d] *Graduate School of Medicine, Hokkaido University, Kita-15, Nishi-7, Kita-Ku, Sapporo 060-8638, Hokkaido, Japan*

ARTICLE INFO

Article history:
Received 8 October 2011
Received in revised form
13 November 2011
Accepted 15 November 2011
Available online 25 November 2011

Keywords:
Hantavirus
Rodent
Genetic diversity
Phylogeny
Mexico

ABSTRACT

A variety of hantaviruses are harbored by rodents in North and South America, some of which can cause hantavirus pulmonary syndrome. To obtain greater evolutionary insight into hantaviruses in the Americas, a total of 211 rodents were captured in the Mexican states of Guerrero and Morelos in 2006. Anti-hantavirus antibodies were detected in 27 of 211 serum samples (12.8%) by ELISA. The distribution of seropositive rodents was: 17 *Peromyscus beatae*, 1 *Megadontomys thomasi*, 1 *Neotoma picta*, 6 *Reithrodontomys sumichrasti*, and 2 *Reithrodontomys megalotis*. The hantavirus small (S), medium (M), and large (L) genome segments from *P. beatae*, *R. sumichrasti*, and *R. megalotis* were amplified and the sequences covering the open reading frames were determined. The hantaviruses from *P. beatae*, *R. sumichrasti*, and *R. megalotis* were provisionally designated Montano (MTN), Carrizal (CAR), and Huitzilac (HUI), respectively. The M segment amino acid identities among the Mexican hantaviruses were 80.8–93.0%. When these M segments were compared to those of known hantaviruses, MTN virus was most closely related to Limestone Canyon (LSC) virus (88.9% amino acid identity), while the CAR and HUI viruses were most closely related to El Moro Canyon (ELMC) virus (90–91% identity). Phylogenetic analysis revealed that the MTN, CAR, and HUI viruses occupy a monophyletic clade with the LSC, ELMC, and Rio Segundo viruses, which are harbored by *Peromyscus boylii*, *R. megalotis*, and *Reithrodontomys mexicanus*, respectively. The data obtained in this study provide important information for understanding the evolution of hantaviruses in the Americas.

1. Introduction

Hantaviruses, which comprise the genus *Hantavirus* in the family *Bunyaviridae*, contain a three-segment negative-sense RNA genome. Small (S), medium (M), and large (L) RNA segments encode the nucleocapsid protein (N), glycoproteins (Gn and Gc), and an RNA-dependent RNA polymerase, respectively (Schmaljohn et al., 1986). Hantaviruses are carried by a variety of rodents and soricomorph species in nature and persistently infect their natural hosts (Jonsson et al., 2010; Song et al., 2007). Some rodent-borne hantaviruses cause hantavirus infections in humans, including hemorrhagic fever with renal syndrome (HFRS) and hantavirus pulmonary syndrome (HPS) (Peters et al., 1999; Schmaljohn and Hjelle, 1997). HFRS, which is characterized by a high fever, hemorrhage, and renal dysfunction with a fatality rate <10%, is distributed throughout Europe, Russia, China, and Korea. HPS, which is characterized by a high fever, pulmonary dysfunction, and cardiac shock and has a ~40% fatality rate (Peters and Khan, 2002), is distributed in North and South Americas. Humans acquire the infection primarily by the inhalation of virus-containing rodent excreta or by the bite of infected animals (Lee and Johnson, 1982). An important characteristic of hantavirus is the close relationship between the virus and its rodent host species, and co-evolution between them may have occurred on a geological timescale (Plyusnin and Morzunov, 2001).

Since the identification of HPS in the United States of America, patients have been reported from various countries in both North and South America; more than 30 hantaviruses have been

* Corresponding author. Tel.: +81 11 706 5212; fax: +81 11 706 5213.
E-mail address: kariwa@vetmed.hokudai.ac.jp (H. Kariwa).

0168-1702/$ – see front matter © 2011 Elsevier B.V. All rights reserved.
doi:10.1016/j.virusres.2011.11.013